J. Phys. B: At. Mol. Opt. Phys. **33** (2000) 971–999. Printed in the UK PII: S0953-4075(00)06100-9

Excitation of autoionizing states of helium by 100 keV proton impact: II. Excitation cross sections and mechanisms of excitation

A L Godunov†, P B Ivanov‡, V A Schipakov‡, P Moretto-Capelle§, D Bordenave-Montesquieu§ and A Bordenave-Montesquieu§

† Department of Physics, Tulane University, New Orleans, LA 70118-5698, USA
‡ Troitsk Institute of Innovation and Fusion Research Troitsk, Moscow region, 142092, Russia
§ Laboratoire Collisions, Agrégats, Réactivité, IRSAMC, UMR 5589, CNRS-Université Paul Sabatier, 31062 Toulouse Cédex, France

Received 19 July 1999, in final form 14 December 1999

Abstract. Mechanisms of two-electron excitation of the $(2s^2)^1S$, $(2p^2)^1D$ and $(2s2p)^1P$ autoionizing states of helium are studied both experimentally and theoretically. It is shown that an explicit introduction of a kinematic factor, with a process-specific phase leads to a productive parametrization of experimental cross sections of ionization, allowing one to extract cross sections of excitation of autoionizing states. Using a new fitting procedure together with the proposed parametrization made it possible to obtain the excitation cross sections and magnetic sublevel population from electron spectra as well as, for the first time, to resolve the contribution of resonance and interference components to resonance profiles. Interference with direct ionization is shown to contribute significantly into resonance formation even for backward ejection angles. We demonstrate theoretically that the excitation cross sections thus extracted from experimental electron spectra hold information about the interaction of autoionizing states with an adjacent continuum.

1. Introduction

The physical nature of autoionizing states lying above the ionization threshold is still not clear enough. Traditionally, in atomic physics, only states with real energies have been considered as true physical states, while any energy broadening has been attributed to interaction with external particles or fields. From this point of view, autoionizing states (AIS) cannot be treated as physical states, since they cannot belong to either the discrete or the continuous spectrum, because their decay does not require any additional external interactions, but predominantly occurs due to internal interactions within the atomic system. The classical theory of resonances (Breit and Wigner 1936), widely used in atomic and nuclear collisions, introduced the idea of a complex-energy state. This theory associates the position of the resonance with the real part of the resonant state energy, and relates the intensity of the resonance to the cross section of the resonant state excitation. However, this model can rarely be applied to autoionizing resonances in photoionization, electron–atom and ion–atom collisions. Since excitation and non-radiative decay of autoionizing states is coherent with direct ionization, the amplitudes of resonant and direct ionization should be summed rather than the probabilities for the two processes, which often changes the resonance shape and intensity. Formally, an autoionizing state can be characterized by a linear combination of both discrete- and continuous-spectrum

0953-4075/00/050971+29$30.00

components, which is not an eigenfunction of a Hermitian operator (see the appendix), or, alternatively, an eigenfunction of a non-Hermitian operator related to the physical Hamiltonian of the system by a complex transformation (Mandl 1966, Reed and Simon 1978, Junker 1985); such 'wavefunctions' do not produce any observables, in the standard interpretation. However, having nearly the same position and width in different collision processes, AIS appear to be more a feature of atomic structure than a property of atomic reactions, and one might wonder whether considering such states may have physical meaning.

There are two approaches in atomic theory that address this question differently. *Close-coupling* calculations do not consider AIS as true physical states, merely modelling the resonance behaviour of the full (continuous-spectrum) wavefunction by introducing various pseudostates (Burke 1965). In contrast, in *configuration-interaction* calculations, AIS are generally treated as truly physical discrete-spectrum states 'embedded' in the continuum. Since excitation and non-radiative decay of such states is coherent with direct ionization, the amplitudes rather than probabilities of resonant and direct ionization must be summed. This leads to their interference, generally resulting in an asymmetric resonance shape, exhibiting both the maximum and minimum being shifted from the resonance position (Fano 1961). The width of the resonance is no longer related to the width of a single peak, and the intensity of the resonance is no longer proportional to the population number of the resonant state (Åberg and Howat 1982). Instead, one has to deal with additional resonance shape parameters, such as the profile index q in Fano's theory, or the asymmetry A and yield B parameters in the Shore formula (Shore 1968), which essentially depend on the type of collision and hence cannot describe atomic structure consistently. The total resonant yield can only provide a lower estimate for the excitation cross section at asymptotic collision velocities (Godunov *et al* 1997a), so that AIS excitation cannot be uncoupled from direct ionization, and the existence of AIS as true atomic states might seem doubtful.

This paper presents evidence that the cross sections of AIS excitation can be extracted from experimental data under certain conditions, and hence it is still possible to consider AIS as physically meaningful atomic states, since their physical characteristics are measurable despite their complex nature. Once measured in a specific reaction, the values obtained can be applied to other collision processes with the same projectile, to uncouple AIS excitation from decay. In this way, one can study the interference of direct and resonant ionization in more detail.

We employ high-resolution electron spectroscopy of autoionizing and Auger resonances excited in fast ion–atom collisions, which has proved to be a powerful method of atomic structure research (Stolterfoht 1987). However, a high-quality experimental set-up, good counting rate and high energy and angular resolution have to be combined with an appropriate theoretical model of resonance phenomena, to allow the extraction of physically meaningful data from experimental spectra.

In collisions with charged projectiles, the Coulomb interaction in the final state (CIFS) between the scattered particle, ejected electron and residual ion can strongly influence both direct ionization (Crooks and Rudd 1970) and resonance profiles in electron emission spectra (Schowengerd and Rudd 1972, Bordenave-Montesquieu *et al* 1975, Arcuni and Schneider 1987, Moretto-Capelle *et al* 1996, Godunov *et al* 1997c). To reproduce experimentally measured spectra, the description of the three-body Coulomb interaction of charged particles in the ionization continuum must be as accurate as the description of two-electron excitation (Godunov *et al* 1997c). This is a challenging problem to both theory and experiment because of additional spectral features significantly complicating the analysis. In the conditions of strong CIFS, resonance profiles may be very different from the familiar Fano shape (Arcuni and Schneider 1987, Moretto-Capelle *et al* 1996), and the traditional Fano or Shore parametrization cannot be applied. The attempts to remove the discrepancies between theory and experiment

by just shifting and broadening the resonance become meaningless if the resonance is split due to the three-body interaction in the final state. Hence, the idea of a PCI shift (Barker and Berry 1966, Kuchiev and Scheinerman 1988) is only applicable for weak Coulomb interactions in the final state.

Progress in this area has recently been achieved in a joint theoretical and experimental study of the excitation of the autoionizing $(2s^2)^1S$, $(2p^2)^1D$ and $(2s2p)^1P$ states of helium by 100 keV proton impact (Godunov *et al* 1997c; hereafter referred to as I). New high-resolution (up to 68 meV) measurements of electron emission spectra made it possible to resolve the near-lying $(2p^2)^1D$ and $(2s2p)^1P$ resonances and reveal an evident distortion of the resonance profiles by CIFS for forward electron ejection angles below 40°. For larger emission angles the resonance lineshape is close to a Fano profile. A new parametrization of resonance profiles, developed on the basis of a three-body model, provided adequate processing of experimental data. When the influence of CIFS is weak, the usual Shore parameters are reproduced as a limiting case for the generalized formula. However, CIFS was found to influence the resonance parameters even in the backward direction. This means that, for an adequate interpretation of experimental data, CIFS should be taken into account for all angles in this region of collision velocities. Considering the complexity of the problem the results of the calculations including CIFS in both the resonant and direct ionization channels and allowing for the second-order terms in the two-electron excitation amplitude agree well with the measurements for all three autoionizing states.

Despite considerable progress in paper I in understanding the role of CIFS in the formation of the autoionizing resonances of helium in electron emission spectra, advancement towards gaining a deeper insight into mechanisms of double excitation and the interplay between resonance and direct transitions demanded additional studies. The new parametrization including CIFS employed five parameters (resonance position, resonance width and three shape parameters), thus extending the usual four-parameter Shore and Fano parametrizations. However, in paper I the fit processing of electron spectra which was used did not allow one to extract meaningful values for all five parameters, especially for the parameter that has a link to the cross section of the excitation of the autoionizing states. It was also not clear to what extent such cross sections contain information about the interaction of autoionizing states with the adjacent continuum. It is the purpose of this paper to address these questions. Preliminary results were published in our recent paper (Moretto-Capelle *et al* 1997).

Here we present a comprehensive experimental and theoretical analysis of the excitation of autoionizing states of helium by 100 keV proton impact, which is used to illuminate a number of important theoretical issues. The new parametrization of resonance profiles distorted by CIFS, as introduced in I, is shown to be a special case of a general approach, and its relation to the Shore parametrization and other parametric expressions is discussed, extending the discussion already given in I. The paper is organized as follows. Section 2 introduces a general procedure allowing one to separate the excitation of autoionizing states from their interference with the continuum. Section 3 demonstrates how these general formulae apply to proton impact ionization of helium. Section 4 gives a brief discussion of the applicability of alternative parametrizations in theory and experiment. In section 5, we describe a new fitting procedure for the processing of the high-resolution spectra measured in I. In section 6 our computational model is briefly recalled. Finally, section 7 contains the results of detailed calculations, experimental measurements and their interpretation and resonance parameters, AIS excitation cross sections and relative phase between resonant and direct ionization transitions are discussed. The appendix presents the technical details of constructing wavefunctions and amplitudes in the diagonalization approach, thus defining the cross section of excitation of autoionizing states that can be extracted from experiments.

2. General parametrizations

2.1. Cross section in the resonance region

In this section, we consider the general case of single ionization of an atomic target by some external perturbation (collision with a charged particle, photoionization or any other projectile), with a perturbation strong enough to allow the formation of autoionization states. That is, the transition from the initial state to a final state may either be direct or involve multiple excitation of the target with subsequent decay of the excited states into the same continuum. We will describe the final state of the system (atomic core + ejected electron + scattered projectile) with the total energy E and a collection of other quantum numbers, a (discrete or continuous), necessary to uniquely identify the state. As discussed in Godunov *et al* (1997a), ionization cross sections for many physically interesting situations can be expressed through a transition amplitude as

$$\sigma(a, E) = C\,|t(a, E)|^2 \tag{1}$$

where the transition amplitude $t(a, E)$ contains singularities

$$t(a, E) = t_{\mathrm{dir}}(a, E) + \sum_{\mu} \frac{t_{\mathrm{res},\mu}(a, E)}{E - E_\mu(a, E) + \mathrm{i}\Gamma_\mu(a, E)/2} \tag{2}$$

with the amplitude $t_{\mathrm{dir}}(a, E)$ describing direct ionization and each term in the sum over μ introducing an autoionization resonance. The form (2) of the transition amplitude implies that the decay of the autoionizing states is close to exponential, so that all the non-exponential dependence can be introduced through the energy dependence of $t_{\mathrm{res},\mu}(a, E)$, $E_\mu(a, E)$ and $\Gamma_\mu(a, E)$. A detailed derivation of the continuum wavefunction and the expression for the transition amplitude can be found in the appendix.

Combining equations (2) and (1), one may easily obtain

$$\sigma(a, E) = \sigma_{\mathrm{dir}}(a, E) + \sum_{\mu} \frac{A_\mu(a, E)\varepsilon_\mu(a, E) + B_\mu(a, E)}{\varepsilon_\mu^2(a, E) + 1} \tag{3}$$

with $\varepsilon_\mu(a, E) = (E - E_\mu(a, E))/\frac{1}{2}\Gamma_\mu(a, E)$, where

$$\sigma_{\mathrm{dir}}(a, E) = C\,|t_{\mathrm{dir}}(a, E)|^2 \tag{4}$$

$A_\mu(a, E)$ and $B_\mu(a, E)$ being the linear combinations of the products $t_{\mathrm{res},\mu}(a, E)t_{\mathrm{res},\nu}(a, E)$ and $t^*_{\mathrm{dir}}(a, E)t_{\mathrm{res},\mu}(a, E)$ with the coefficients expressible through $\varepsilon_{\mu\nu}(a, E) = (E_\mu(a, E) - E_\nu(a, E))/\frac{1}{2}\Gamma_{\mu\nu}(a, E)$ and $\Gamma_{\mu\nu}(a, E) = \Gamma_\mu(a, E) + \Gamma_\nu(a, E)$ (Ivanov 1989, I). Equation (3) was originally derived by Shore (1968) for the most general case of an atom interacting with radiation; however, equation (3) is valid for the cross sections of any other ionization process, involving an arbitrary number of interfering autoionization states decaying into any number of ionization channels, coupled by any kind of atomic interaction.

In the physically important case of isolated resonances, the parameters in (3) can be expressed as (Godunov *et al* 1997a)

$$A_\mu(a, E) = \frac{4C}{\Gamma_\mu(a, E)}\,\mathrm{Re}(t^*_{\mathrm{dir}}(a, E)t_{\mathrm{res},\mu}(a, E)) \tag{5}$$

$$B_\mu(a, E) = \frac{4C}{\Gamma_\mu(a, E)}\left\{\mathrm{Im}(t^*_{\mathrm{dir}}(a, E)t_{\mathrm{res},\mu}(a, E)) + \frac{1}{\Gamma_\mu(a, E)}\left|t_{\mathrm{res},\mu}(a, E)\right|^2\right\} \tag{6}$$

Though the following discussion does not depend on the isolatedness of the resonances and the same results could be obtained in the general case as well (see I), the approximation (equations (5) and (6)) seems to provide a good illustration of the principal ideas without too much technical complexity.

2.2. Energy dependence of the resonance parameters

The pole singularity is analytically separated in formula (3), so the rest of the energy dependence is encapsulated in the coefficient functions $A_\mu(a, E)$, $B_\mu(a, E)$, $E_\mu(a, E)$, $\Gamma_\mu(a, E)$. Various cases of energy dependence are encountered.

The *simplest assumption* would be that A_μ and B_μ as well as E_μ and Γ_μ are constant in the resonance region. Most theoretical and experimental works on atomic ionization rely on this approximation, which has proved quite satisfactory in low-energy photoabsorption problems. However, already for the photoionization of atoms via autoionizing states converging to higher ionization thresholds, when the problem becomes essentially multichannel, the deviation from parametrization (3) with constant A_μ and B_μ becomes significant, which led some physicists to model the variation of the fitting coefficients with energy in a wider range by their linear or quadratic expansions in powers of ε_μ (Ivanov and Senashenko 1983, Ivanov 1989). On the other hand, in the collisions of charged particles with atomic targets, Coulomb interactions in the final state have been known for a long time to significantly influence the profiles of autoionization resonances (Schowengerdt and Rudd 1972, Bordenave-Montesquieu *et al* 1975, Heideman and van de Water 1981, Arcuni and Schneider 1987), resulting even in a deviation of resonance profiles from the Fano shape (Arcuni and Schneider 1987, Moretto-Capelle *et al* 1996). The effect is more pronounced in differential cross sections. A semiempirical attempt to account for post-collision interaction through introducing a resonance shift (Barker and Berry 1966, Kuchiev and Scheinerman 1988) could only have a limited applicability (weak CIFS), giving little new information about the physical mechanisms involved.

To reveal more details in the general picture of resonant ionization, one has to consider a *more specific energy dependence* of the coefficient functions $A_\mu(a, E)$ and $B_\mu(a, E)$ in (3). An intuitively appealing approach has been suggested in I, where the influence of CIFS on the resonance ionization channel has been factored out as a complex factor

$$t_{\mathrm{res},\mu}(a, E) = \beta_\mu(a, E)\, \mathrm{e}^{\mathrm{i}\alpha_\mu(a,E)} t^0_{\mathrm{res},\mu}(a) \tag{7}$$

so that

$$t(a, E) = t_{\mathrm{dir}}(a, E) + \sum_\mu \frac{\beta_\mu(a, E)\, \mathrm{e}^{\mathrm{i}\alpha_\mu(a,E)} t^0_{\mathrm{res},\mu}(a)}{E - E_\mu(a) + \mathrm{i}\Gamma_\mu(a)/2}. \tag{8}$$

Equation (8) agrees with the general principle of quantum scattering theory that virtual interactions in the system must be asymptotically represented by a process-specific phase; for instance, such a phase shift may be a consequence of the scattered projectile's influence on the decay of the autoionizing state (post-collision interaction). The exact form of functions $\beta_\mu(a, E)$ and $\alpha_\mu(a, E)$ depends both on the level of the description of the particles involved (target, projectile, ejected electron) and on the adopted level of distinction between pre- and post-collision interactions.

If the dominant part of the energy dependence in (8) is contained in the resonance amplitude, then substituting (7) into (5) and (6), one can obtain

$$A_\mu(a, E) = \beta_\mu(a, E)\left[A_{\mathrm{int},\mu}(a)\cos\alpha_\mu(a, E) - B_{\mathrm{int},\mu}(a)\sin\alpha_\mu(a, E)\right] \tag{9}$$

$$B_\mu(a, E) = \beta_\mu(a, E)[A_{\mathrm{int},\mu}(a)\sin\alpha_\mu(a, E) + B_{\mathrm{int},\mu}(a)\cos\alpha_\mu(a, E) + B_{\mathrm{exc},\mu}(a)\beta_\mu(a, E)] \tag{10}$$

with

$$A_{\mathrm{int},\mu}(a) = \frac{4C}{\Gamma_\mu(a)}\,\mathrm{Re}(t^*_{\mathrm{dir}}(a) t^0_{\mathrm{res},\mu}(a)) \tag{11}$$

$$B_{\mathrm{int},\mu}(a) = \frac{4C}{\Gamma_\mu(a)} \operatorname{Im}(t^*_{\mathrm{dir}}(a) t^0_{\mathrm{res},\mu}(a)) \tag{12}$$

$$B_{\mathrm{exc},\mu}(a) = \frac{4C}{\Gamma^2_\mu(a)} \left| t^0_{\mathrm{res},\mu}(a) \right|^2 . \tag{13}$$

As demonstrated in Godunov *et al* (1997a) and Moretto-Cappele *et al* (1997), the parameter $B_{\mathrm{exc},\mu}(a)$ can be reduced to the product $\Gamma_\mu \sigma_{\mathrm{exc},\mu}$, where $\sigma_{\mathrm{exc},\mu}$ is the cross section of the excitation of the autoionizing state μ. One can expect that the peculiar kind of energy dependence of the coefficient functions $A_\mu(a, E)$ and $B_\mu(a, E)$ specified by equations (9) and (10) may give the clue to experimentally determining the excitation cross section. Indeed, accounting for (9), (10), equation (3) can be rewritten as

$$\sigma(a, E) = \sigma_{\mathrm{dir}}(a, E) + \sum_\mu \frac{\beta_\mu(a\varepsilon_\mu)}{\varepsilon^2_\mu + 1} \times [A_{\mathrm{int},\mu}(a) f_1(a\varepsilon_\mu) + B_{\mathrm{int},\mu}(a) f_2(a\varepsilon_\mu) + B_{\mathrm{exc},\mu}(a) f_3(a\varepsilon_\mu)] \tag{14}$$

where

$$f_1(a\varepsilon_\mu) = \varepsilon_\mu \cos\alpha_\mu(a\varepsilon_\mu) + \sin\alpha_\mu(a\varepsilon_\mu) \tag{15}$$

$$f_2(a\varepsilon_\mu) = \cos\alpha_\mu(a\varepsilon_\mu) - \varepsilon_\mu \sin\alpha_\mu(a\varepsilon_\mu) \tag{16}$$

$$f_3(a\varepsilon_\mu) = \beta_\mu(a\varepsilon_\mu). \tag{17}$$

Equation (14) can also be obtained directly from equations (1) and (8), by employing the limit of isolated resonances.

2.3. Excitation cross section

If functions f_1, f_2 and f_3 contain the dominant part of the energy dependence in (14) one could use equation (14) as a parametric formula in interpreting ionization spectra. Knowing the values of $B_{\mathrm{exc},\mu}$ and Γ_μ thus obtained, one can derive the value of $\sigma_{\mathrm{exc},\mu}$.

A number of general conditions must be satisfied to make such an indirect measurement possible. Thus, for weakly coupled systems, $\beta_\mu \simeq 1$ and $\alpha_\mu \simeq 0$, so that (14) reduces to the usual Shore parametrization with $B_\mu = B_{\mathrm{int},\mu} + B_{\mathrm{exc},\mu}$, and the excitation of autoionization states cannot be separated from their interaction with the continuum and decay. This limit has been studied extensively in I. It should be stressed that equation (14) must be considered as a special case of Shore's formula (3) with energy-dependent coefficients; in contrast, Shore parametrization with constant coefficients appears to be a special case of the more general parametrization (14). The assumption of constant parameters is just another constraint on the energy dependence of the cross section, and it is well known that a constraint on a general formula is stronger than the same constraint applied to a part of it.

We note that post-collision interaction must be strong enough to allow the splitting of the coefficient B_μ into interference and excitation parts. This implies a strong distortion of the classical resonance shape as described by Shore (or equivalent Fano) parametrization with constant coefficients. For a rapid variation of α_μ with energy near resonance, this distortion cannot be reduced to a mere resonance shift, the oscillatory behaviour of $\sin\alpha_\mu$ and $\cos\alpha_\mu$ resulting in additional extrema producing the effect of resonance splitting. With the phase separation in (7) reflecting the kinematics of the problem, this effective splitting may have, in the case of a charged projectile impact, much in common with the dynamic Stark effect. A detailed investigation of this relation goes beyond the scope of this paper. However, we can note that the perturbation from the projectile must be essentially non-stationary to allow separation

of $B_{\mathrm{int},\mu}$ and $B_{\mathrm{exc},\mu}$—otherwise, it would result in a mere energy shift and broadening with nearly constant phase, which returns us to the Shore formula.

To be suited for reliably extracting AIS excitation cross sections from experimental spectra, functions f_1 and f_2 must both be nearly orthogonal in energy to f_3 in the resonance region. For instance, for α_μ linear in energy and slow-varying β_μ, terms with f_1 and f_2 in (14) give the sine and cosine first-order components of a Fourier series, with the zero-order term f_3 being automatically orthogonal to them. In general, any two of these functions may overlap; the respective parameters would sum up in that case, with information loss. Simultaneously fitting experimental spectra for a few values of the parameters a that exhibit different energy behaviour of f_1, f_2 and f_3 would significantly improve the accuracy of the fitted parameters. Therefore, differential cross sections provide a better source of data for indirect measurement of AIS excitation cross sections, while integral cross sections leave too few parameters to control.

3. Ionization by charged particle impact

As an illustration of the general assertions of the previous subsection, we consider the problem of ionization of an atomic target in collisions with a charged particle. A solution of a three-particle problem for the interaction of the scattered projectile, ejected electron and recoil ion in the final state gives the transition amplitude as (Godunov *et al* 1989, I)

$$t(a, E) = K_{\mathrm{dir}}(a, E)t^{\mathrm{b}}_{\mathrm{dir}} + \sum_{\mu} K_{\mathrm{res},\mu}(a, E)\frac{t^{0}_{\mathrm{dec},\mu}t_{\mathrm{exc},\mu}}{E - E_\mu + \mathrm{i}\Gamma_\mu/2} \tag{18}$$

where $t^{\mathrm{b}}_{\mathrm{dir}}$ is the direct ionization amplitude in the Born approximation, $t^{0}_{\mathrm{dec},\mu}$ is the amplitude for non-radiative decay of an autoionizing state in an isolated atom, $t_{\mathrm{exc},\mu}$ is the excitation amplitude for the autoionizing state μ, and E_μ, Γ_μ are the resonance position and resonance width, respectively. $K_{\mathrm{dir}}(a, E)$ and $K_{\mathrm{res},\mu}(a, E)$ are the factors allowing for CIFS in the direct and resonance ionization amplitudes; their explicit form can be found elsewhere (Godunov *et al* 1989, I). Equation (18) is a special case of equation (2), with

$$t_{\mathrm{dir}}(a, E) = K_{\mathrm{dir}}(a, E)t^{\mathrm{b}}_{\mathrm{dir}} \tag{19}$$

$$t_{\mathrm{res},\mu}(a, E) = K_{\mathrm{res},\mu}(a, E)t^{0}_{\mathrm{dec},\mu}t_{\mathrm{exc},\mu}. \tag{20}$$

In the kinematic region considered, one can use the eikonal limit of the above expressions, obtaining (for details see I) for the functions in equation (7),

$$\beta_\mu(a, E) = \exp(-\xi \arctan \varepsilon_\mu) \tag{21}$$

$$\alpha_\mu(\varepsilon_\mu) = -\xi \ln(\varepsilon_\mu^2 + 1)/2 \tag{22}$$

with

$$\xi = \frac{Z_{\mathrm{p}}}{v_{\mathrm{f}}}\left(Z_{\mathrm{t}} - \frac{v_{\mathrm{f}}}{v_{\mathrm{pe}}}\right) \tag{23}$$

where Z_{p} and Z_{t} are the charges for the projectile and the recoil ion accordingly, v_{f} is the velocity of the scattered particle, v_{pe} is the relative velocity in final state between the scattered particle and the ejected electron. And the double differential cross section of ionization can

be written as (Godunov *et al* 1992, I)

$$\frac{\mathrm{d}^2\sigma}{\mathrm{d}E_\mathrm{e}\,\mathrm{d}\Omega_\mathrm{e}} = F(E_\mathrm{i}, E_\mathrm{e}, \theta_\mathrm{e}) + \sum_\mu \frac{\exp(-\xi \arctan \varepsilon_\mu)}{\varepsilon_\mu^2 + 1} \times\{A_{\mathrm{int},\mu}(E_\mathrm{i}, \theta_\mathrm{e})[\varepsilon_\mu \cos(\alpha_\mu(\varepsilon_\mu)) + \sin(\alpha_\mu(\varepsilon_\mu))] + B_{\mathrm{int},\mu}(E_\mathrm{i}, \theta_\mathrm{e})[\cos(\alpha_\mu(\varepsilon_\mu)) - \varepsilon_\mu \sin(\alpha_\mu(\varepsilon_\mu))] + B_{\mathrm{exc},\mu}(E_\mathrm{i}, \theta_\mathrm{e}) \exp(-\xi \arctan \varepsilon_\mu)\}. \tag{24}$$

The parameters in equation (24) are determined as

$$A_{\mathrm{int},\mu}(E_\mathrm{i}, \theta_\mathrm{e}) = (2\pi)^4 m_\mathrm{p}^2 \frac{K_\mathrm{f} k_\mathrm{e}}{K_\mathrm{i}} 2\,\mathrm{Re}\left\{K^0_{\mathrm{res},\mu} \int \mathrm{d}\Omega_\mathrm{f} (t^*_\mathrm{dir} t_{\mathrm{dec},\mu} t_{\mathrm{exc},\mu})\right\} \tag{25}$$

$$B_{\mathrm{int},\mu}(E_\mathrm{i}, \theta_\mathrm{e}) = (2\pi)^4 m_\mathrm{p}^2 \frac{K_\mathrm{f} k_\mathrm{e}}{K_\mathrm{i}} 2\,\mathrm{Im}\left\{K^0_{\mathrm{res},\mu} \int \mathrm{d}\Omega_\mathrm{f} (t^*_\mathrm{dir} t_{\mathrm{dec},\mu} t_{\mathrm{exc},\mu})\right\} \tag{26}$$

$$B_{\mathrm{exc},\mu}(E_\mathrm{i}, \theta_\mathrm{e}) = (2\pi)^4 m_\mathrm{p}^2 \frac{K_\mathrm{f} k_\mathrm{e}}{K_\mathrm{i}} \left|K^0_{\mathrm{res},\mu}\right|^2 \int \mathrm{d}\Omega_\mathrm{f} \left|t_{\mathrm{dec},\mu} t_{\mathrm{exc},\mu}\right|^2 \tag{27}$$

where K_i and K_f are the momenta of the incoming and outgoing projectile, k_e is the momenta of the ejected electron, m_p is the mass of the projectile and $\mathrm{d}\Omega_\mathrm{f}$ is the solid angle element in the direction of the scattered projectile's velocity. Obviously, equations (25)–(27) are a special case of equations (11)–(13), the integrals representing a partial summation over the configuration indices a.

Separating out the angular dependence of the amplitude $t_{\mathrm{dec},\mu}$, one can link the parameter $B_{\mathrm{exc},\mu}(E_\mathrm{i}, \theta_\mathrm{e})$ to the cross section of the excitation of the autoionizing state μ. Indeed, the amplitude of the non-radiative decay $t_{\mathrm{dec},\mu}$ of an autoionizing state with the total orbital momentum L can be written as (I)

$$t_{\mathrm{dec},\mu} = \frac{2}{\Gamma_\mu} \mathrm{i}^L \exp(\mathrm{i}\delta_L) \tau_{\mathrm{dec},\mu} Y_{LM}(\Omega_\mathrm{e}) \tag{28}$$

where δ_L is the phase of the continuum wavefunction and the amplitude $\tau_{\mathrm{dec},\mu}$ determines the resonance width in an isolated atomic system

$$\Gamma_\mu = 2\pi \left|\tau_{\mathrm{dec},\mu}\right|^2. \tag{29}$$

Substituting these expressions into equation (27) and accounting for

$$\left|K^0_{\mathrm{res},\mu}\right| = \frac{\pi\xi}{\sinh(\pi\xi)} \tag{30}$$

one obtains

$$\tfrac{1}{2}(\pi\Gamma_\mu) B_{\mathrm{exc},\mu}(E_\mathrm{i}, \theta_\mathrm{e}) \frac{\sinh(\pi\xi)}{\pi\xi} = \sum_{M=-L}^{L} \sigma^{LM}_{\mathrm{exc},\mu} P^2_{LM}(\cos\theta_\mathrm{e}) \tag{31}$$

where $P_{LM}(\cos\theta_\mathrm{e})$ is the associated Legendre function and $\sigma^{LM}_{\mathrm{exc},\mu}$ denotes the cross section of the target excitation to the state with total orbital momentum L and magnetic sublevel M. The total AIS excitation cross section is given by

$$\sigma_\mathrm{exc}(E_\mathrm{i}) = \sum_{M=-L}^{L} \sigma^{LM}_\mathrm{exc}(E_\mathrm{i}) = (2\pi)^4 m_\mathrm{p}^2 \frac{K_\mathrm{f}}{K_\mathrm{i}} \sum_{M=-L}^{L} \int \left|t^{LM}_{\mathrm{exc},\mu}\right|^2 \mathrm{d}\Omega_\mathrm{f}. \tag{32}$$

That is, knowing the angular dependence of the resonance parameter $B_{\mathrm{exc},\mu}(E_\mathrm{i}, \theta_\mathrm{e})$ from fitting experimental spectra to the formulae (14) or (24), one can derive the cross sections $\sigma_\mathrm{exc}(E_\mathrm{i})$ and $\sigma_\mathrm{exc}^{LM}(E_\mathrm{i})$ for the excitation of the autoionizing state.

We stress once again that separating out the excitation part of the B_μ coefficient does not mean that there is no interference between the direct and resonant ionization; on the contrary, one has to add interactions between the ejected electron, residual ion and scattered projectile to achieve that separability. As shown in the appendix, this means more correlation in the continuum, with all the discrete–continuum interference preserved.

4. Other parametric formulae

While Shore parametrization (3) contains two profile parameters for each resonance, parametrization (14) introduces three parameters for each resonance. However, additional parameters cannot guarantee the possibility of extracting new physical information by themselves. One also has to relate theoretically the parameters to some quantities possessing a clear physical sense. Thus, the semiempirical approximation of the energy dependence of the coefficient functions $A_\mu(a, E)$ and $B_\mu(a, E)$ in (3) by polynomials in ε_μ may be quite efficient for the quantitative description of experimental spectra, but it gives little for understanding the physics of autoionization, and it is bound to fail to describe some important features arising from the non-analytic behaviour of the transition amplitude (e.g. cusps). Still, phenomenological formulae like that may be useful for applications requiring large banks of atomic data (Godunov and Ivanov 1999).

A different kind of many-parameter formulae is known in the theory of partial cross sections of resonant ionization. Thus, Fano's (Fano 1961) profile index q_p for an isolated resonance in a partial cross section is related to the profile index for the corresponding total cross section q by the expression (Ivanov 1989)

$$q_\mathrm{p} = \tfrac{1}{2}\left[q\delta - (2-q)/\delta\right] + \sqrt{\tfrac{1}{4}\left[q\delta + (2-q)/\delta\right]^2 + (1-q)^2} \tag{33}$$

with an additional dimensionless parameter δ that can either be calculated theoretically or extracted from experimental data for total and partial cross sections; however, since δ is expressed through both the total and partial widths as well as the on-shell parts of the total and partial amplitudes of indirect AIS excitation through the continuum (Godunov *et al* 1997a), extracting more information about the separate amplitudes or phases can only be possible in a few very special cases (Ivanov 1989). One could also recall the well known Starace parametrization for a single-channel cross section in multichannel photoionization (Starace 1977)

$$A_\mu(a, E) = \sigma_\mathrm{dir}(a, E) 2\left[q_\mu \operatorname{Re}\gamma_\mu(a) - \operatorname{Im}\gamma_\mu(a)\right] \tag{34}$$

$$B_\mu(a, E) = \sigma_\mathrm{dir}(a, E)\left\{-2\left[q_\mu \operatorname{Im}\gamma_\mu(a) + \operatorname{Re}\gamma_\mu(a)\right] + (q_\mu^2 + 1)\left|\gamma_\mu(a)\right|^2\right\} \tag{35}$$

closely resembling equations (9) and (10). However, this parametrization encounters the same interpretational problems as formula (33). Since equation (3) holds for any kind of cross section (partial and total, differential and integral), no 'full experiment' (Starace 1977, Krause *et al* 1983) can separate AIS interference with the continuum from AIS excitation, unless there is a strong energy dependence of the relative phase introduced by equation (7). In other words, the processes of excitation and decay of autoionizing states must be essentially influenced by an inhomogeneous external potential with an inhomogeneity length comparable to the size of the excited target, in which case the gross factoring out of direct ionization as in equations (34)

and (35) is impossible. For the proton-impact ionization of helium considered in this paper, the above-mentioned potential is associated with the projectile's current.

Every parametrization may have a number of alternative formulations, which do not introduce a different level of consideration, but rather provide a variety of presentations stressing different aspects of the same theory. Thus, the Shore formula (3) is often rewritten in the Fano–Cooper form (Fano and Cooper 1963)

$$\sigma = \sigma_{\text{dir}} \left\{ \left(1 - \sum_{\mu} \rho_{\mu}^2 \right) + \sum_{\mu} \rho_{\mu}^2 \frac{(\varepsilon_{\mu} + q_{\mu})^2}{\varepsilon_{\mu}^2 + 1} \right\} \tag{36}$$

where functions $q_{\mu} = q_{\mu}(a, E)$ and $\rho_{\mu}^2 = \rho_{\mu}^2(a, E)$ are related to the Shore coefficients by the equations

$$A_{\mu} = 2\rho_{\mu}^2 q_{\mu} \sigma_{\text{dir}} \tag{37}$$

$$B_{\mu} = \rho_{\mu}^2 (q^2 - 1) \sigma_{\text{dir}}. \tag{38}$$

The form (36) is equivalent to (3), being as general. It may be preferable since the parameters q_{μ} and ρ_{μ}^2 are dimensionless, which makes the comparison of different targets simpler. However, it lacks the linearity of equation (3), and the relation between the parameters of various kinds of cross sections becomes less straightforward.

A number of alternative forms can be derived for formula (14) as well. Introducing dimensionless parameters R_{μ} and δ_{μ} with equations

$$A_{\text{int},\mu} = \beta_{\mu} B_{\text{exc},\mu} R_{\mu} \cos \delta_{\mu} \tag{39}$$

$$B_{\text{int},\mu} = \beta_{\mu} B_{\text{exc},\mu} R_{\mu} \sin \delta_{\mu} \tag{40}$$

or, inversely,

$$R_{\mu} = \frac{\sqrt{A_{\text{int},\mu}^2 + B_{\text{int},\mu}^2}}{\beta_{\mu} B_{\text{exc},\mu}} \tag{41}$$

$$\delta_{\mu} = \arctan \frac{B_{\text{int},\mu}}{A_{\text{int},\mu}} + \pi n \qquad (n = 0, 1, \ldots) \tag{42}$$

one can rewrite equation (14) as

$$\sigma = \sigma_{\text{dir}} + \sum_{\mu} \frac{\beta_{\mu}^2 B_{\text{exc},\mu}}{\varepsilon_{\mu}^2 + 1} \left\{ 1 + R_{\mu} [\varepsilon_{\mu} \cos \omega_{\mu} + \sin \omega_{\mu}] \right\} \tag{43}$$

where $\omega_{\mu} = \delta_{\mu} + \alpha_{\mu}$. Thus, for the double-differential cross section of ion-impact ionization of helium considered in the previous section, we obtain

$$\frac{\mathrm{d}^2\sigma}{\mathrm{d}E_{\text{e}}\, \mathrm{d}\Omega_{\text{e}}} = F(E_{\text{i}}, E_{\text{e}}, \theta_{\text{e}}) + \sum_{\mu} \frac{\exp(-2\xi \arctan \varepsilon_{\mu}) B_{\text{exc},\mu}(E_{\text{i}}, \theta_{\text{e}})}{\varepsilon_{\mu}^2 + 1}$$
$$\times \left\{ 1 + R_{\mu}(E_{\text{i}}, \theta_{\text{e}}) \left[\varepsilon_{\mu} \cos \omega_{\mu}(E_{\text{i}}, \theta_{\text{e}}) + \sin \omega_{\mu}(E_{\text{i}}, \theta_{\text{e}}) \right] \right\} \tag{44}$$

with $\omega_{\mu} = \delta_{\mu} - \xi \ln(\varepsilon_{\mu}^2 + 1)/2$. In a slightly different form, this expression has been introduced in Godunov *et al* (1992).

The resonance terms in equation (43) are proportional to $B_{\text{exc},\mu}$ which is related to the AIS excitation cross section; that is, the classical Breit–Wigner form of the resonance becomes factored out, and the whole effect of the autoionizing state's interference with the continuum, including CIFS, is contained in the dimensionless quantities R_{μ} and α_{μ}. This, as in the case

of Fano and Shore parametrizations, may make these parameters more suited for comparing the results for different targets excited by different projectiles. Such dimensionless quantities may also be of importance for investigating the common features of reactions with massive projectiles and photoionization. Since the ratios of measurable quantities do not contain any constant calibration factors, the systematic error introduced through the calibration procedure is eliminated, which makes dimensionless quantities popular among experimentalists too.

5. Fitting procedure

The profiles of the $(2s^2)^1S$, $(2s2p)^1P$ and $(2p^2)^1D$ resonances, measured in I, have been analysed using formula (24). In I this formula was proved to be adequate to reproduce the observed profiles. In that paper each electron spectrum was fitted separately. The structure of relation (24) makes it apparent that for each resonance we have to adjust three parameters $A_{\mathrm{int},\mu}(E_\mathrm{i},\theta_\mathrm{e})$, $B_{\mathrm{int},\mu}(E_\mathrm{i},\theta_\mathrm{e})$ and $B_{\mathrm{exc},\mu}(E_\mathrm{i},\theta_\mathrm{e})$ for each resonance, each of them having its own (unknown) angular dependence. In this way only one electron spectrum can be fitted at once and it appears that no reliable solution can be found for these three parameters; it was observed that only $A_{\mathrm{int},\mu}(E_\mathrm{i},\theta_\mathrm{e})$ and the sum $[B_{\mathrm{int},\mu}(E_\mathrm{i},\theta_\mathrm{e}) + B_{\mathrm{exc},\mu}(E_\mathrm{i},\theta_\mathrm{e})]$ are reliable (as used in I). The difficulties which were encountered can be illustrated in the following way. The possibility to extract all three resonance parameters $A_{\mathrm{int},\mu}(E_\mathrm{i},\theta_\mathrm{e})$, $B_{\mathrm{int},\mu}(E_\mathrm{i},\theta_\mathrm{e})$ and $B_{\mathrm{exc},\mu}(E_\mathrm{i},\theta_\mathrm{e})$ from a fit of experimental electron spectra relies *a priori* on the fact that the functions $f_1(E_\mathrm{i},\theta_\mathrm{e},\varepsilon_\mu)$, $f_2(E_\mathrm{i},\theta_\mathrm{e},\varepsilon_\mu)$ and $f_3(E_\mathrm{i},\theta_\mathrm{e},\varepsilon_\mu)$ in equation (14) have their own specific dependence against the electron energy. In figure 1 we plot the three whole functions $[(f_3(E_\mathrm{i},\theta_\mathrm{e},\varepsilon_\mu)/(\varepsilon_\mu^2+1))f]$, with $f = f_1$, f_2 or f_3 for three angles in regions of strong and small CIFS (10°, 90° and 160°, respectively). These profiles, not convolved by the apparatus function, are given for the S resonance; they are almost the same for the other two resonances, apart from the width, which is smaller in the latter case because of the values of the natural widths Γ_μ. The multiplying factor of $A_{\mathrm{int},\mu}(E_\mathrm{i},\theta_\mathrm{e})$ always has a typical energy dependence which helps us in extracting this parameter at all angles, even with the usual fit as used in I. On the other hand, the multiplying factors of $B_{\mathrm{int},\mu}(E_\mathrm{i},\theta_\mathrm{e})$ and $B_{\mathrm{exc},\mu}(E_\mathrm{i},\theta_\mathrm{e})$ can only be distinguished at forward angles; this means that using the usual fitting procedure only the sum $B_\mu = B_{\mathrm{int},\mu} + B_{\mathrm{exc},\mu}$ can be extracted in the backward direction. Then, if we want to extract all three parameters from the experimental electron spectra, some other procedure should be found to isolate each $B_{\mathrm{int},\mu}$ and $B_{\mathrm{exc},\mu}$ contribution.

Therefore, another fitting method was developed in this paper to extract the values of all three resonance parameters (see also Moretto-Capelle *et al* 1997). Indirectly, we take advantage of the decoupling of $B_{\mathrm{int},\mu}(E_\mathrm{i},\theta_\mathrm{e})$ from $B_{\mathrm{exc},\mu}(E_\mathrm{i},\theta_\mathrm{e})$ in equation (24), compared to the Shore form of the B parameter (6), by using the definition of $B_{\mathrm{exc},\mu}(E_\mathrm{i},\theta_\mathrm{e})$ as given by (31). Relation (31) says that the angular dependence of $B_{\mathrm{exc},\mu}(E_\mathrm{i},\theta_\mathrm{e})$ is known and given by the Legendre polynomial provided that the excitation cross sections $\sigma_{\mathrm{exc}}^{LM}(E_\mathrm{i})$ of the magnetic sublevels are determined. Therefore, instead of extracting the resonance parameter $B_{\mathrm{exc},\mu}(E_\mathrm{i},\theta_\mathrm{e})$ we consider the $\sigma_{\mathrm{exc}}^{LM}(E_\mathrm{i})$ cross sections as new adjustable parameters. At first sight this seems a strange idea since instead of three independent parameters for each resonance, which cannot already be extracted from a single spectrum in a reliable way as just mentioned, we now increase their number through the excitation cross sections of individual magnetic sublevels. The key point is that the sublevel excitation cross sections are independent of the angle and must be the same in the description of any electron spectrum measured at any angle. Therefore, the new fitting procedure which has been used consists in fitting together the maximum number of electron spectra, covering the whole angle range, to put strong constraints on the adjustable parameters: $A_{\mathrm{int},\mu}(E_\mathrm{i},\theta_\mathrm{e})$ and $B_{\mathrm{int},\mu}(E_\mathrm{i},\theta_\mathrm{e})$ are independent adjustable parameters at each

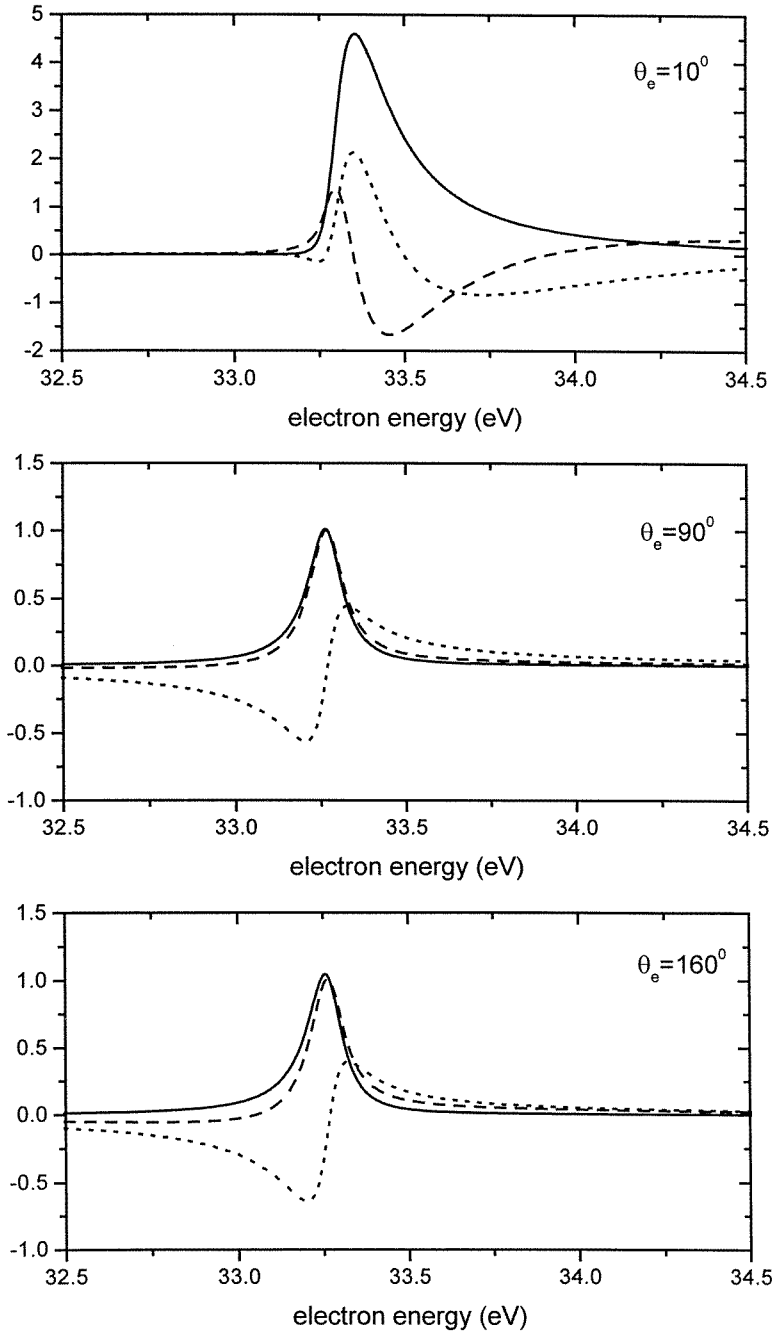

Figure 1. Examples of the electron energy dependence of the factors $[(f_3(E_\mathrm{i}, \theta_\mathrm{e}, \varepsilon_\mu)/(\varepsilon_\mu^2 + 1))f]$, with $f = f_1(E_\mathrm{i}, \theta_\mathrm{e}, \varepsilon_\mu)$, $f_2(E_\mathrm{i}, \theta_\mathrm{e}, \varepsilon_\mu)$ and $f_3(E_\mathrm{i}, \theta_\mathrm{e}, \varepsilon_\mu)$ for $(2s^2)^1$S resonance of helium excited by 100 keV proton impact. Electron emission angles are 10°, 90° and 160°. Full curve, factor for the B_exc parameter; broken curve, factor for the B_int parameter and dotted curve, factor for the A_int parameter from equation (24).

angle, whereas the $\sigma_{\rm exc}^{LM}(E_{\rm i})$ cross sections must fit the whole set of electron spectra. Therefore, the values of $\sigma_{\rm exc}^{LM}(E_{\rm i})$ extracted from forward emission angles help to separate the resonance and interference components in the backward direction (region of small CIFS). The power of the method is thus enhanced. Up to a maximum of 15 spectra were fitted *together*. Various combinations of spectra have been tried, each of them defining a fitting set which always covers the whole angular range. The resonance position E_μ and width Γ_μ were taken from theoretical calculations (see I). The direct ionization cross section $F(E_{\rm i}, E_{\rm e}, \theta_{\rm e})$ was approximated by a first-order polynomial. The resonance parameter $B_{\rm exc}$ has then be deduced from the adjusted $\sigma_{\rm exc}^{LM}$ values using formula (31).

This new fitting method already strongly restricts the variation of the adjustable parameters which can be used. Two additional constraints have been added in the fitting procedure: (a) the excitation cross section $\sigma_{\rm exc}^{LM}(E_{\rm i})$ must be positive; (b) $\sqrt{A_{{\rm int},\mu}(E_{\rm i},\theta_{\rm e})^2 + B_{{\rm int},\mu}(E_{\rm i},\theta_{\rm e})^2} \leqslant 2\sqrt{B_{{\rm exc},\mu}(E_{\rm i},\theta_{\rm e})F(E_{\rm i},E_{\rm e},\theta_{\rm e})}$ where the direct ionization cross section $F(E_{\rm i}, E_{\rm e}, \theta_{\rm e})$ is determined at the resonance position $E_{\rm e} = E_\mu$. The latter condition was simply derived from the definitions of the resonance parameters. The new fitting procedure has been proved to be reliable; it gives stable values of the resonance parameters when different sets of spectra are used; averaged values of the parameters obtained with various combinations of spectra will be considered in the following.

6. Computational model

Our computation model in this work is nearly the same as in I except that most calculations have been carried out with a multi-configuration Hartree–Fock function. However, new collision characteristics have been calculated: cross sections for the double-electron excitation of autoionizing states, resonance parameters $B_{{\rm int},\mu}(E_{\rm i},\theta_{\rm e})$ and $B_{{\rm exc},\mu}(E_{\rm i},\theta_{\rm e})$ separately, relative phase $\delta_\mu(E_{\rm i},\theta_{\rm e})$ between the direct and the resonance ionization.

7. Results

In paper I, we tested the adequacy of the parametrization (24) to describe the observed lineshapes in the kinematic conditions under investigation. It succeeded in reproducing all the measured lineshapes. We focused on the influence of CIFS on the following two resonance parameters $A_{{\rm int},\mu}(E_{\rm i},\theta_{\rm e})$ and $B_\mu(E_{\rm i},\theta_{\rm e}) = B_{{\rm int},\mu}(E_{\rm i},\theta_{\rm e}) + B_{{\rm exc},\mu}(E_{\rm i},\theta_{\rm e})$. The importance of second-order terms in the calculated excitation amplitudes was also stressed. In this paper, we apply the new fitting procedure described above to the high-resolution electron spectra in the vicinity of the low-lying autoionizing $(2s^2)^1$S, $(2s2p)^1$P and $(2p^2)^1$D states of helium excited by 100 keV proton impact for emission angles between 10° and 160°, comparing the results with our theoretical calculations for the three resonance parameters $A_{\rm int}$, $B_{\rm int}$ and $B_{\rm exc}$ as well as the two-electron excitation cross sections $\sigma_{\rm exc}^{LM}$.

7.1. Resonance profiles

The extraction of the two groups of resonance parameters from electron spectra in the conditions of strong CIFS, $A_{\rm int}$ and $B_{\rm int}$, on one hand, and $B_{\rm exc}$, on the other hand, allows us to investigate the relative contributions of the interference and excitation terms, respectively, to the internal structure of the observed resonance profiles. Since excitation cross sections do not depend on the electron emission angle, we can use the values of $B_{\rm exc}$ extracted from forward-emission data to also separate the resonance and interference components in the region of small CIFS (e.g. for backward emission), where normally one could only obtain $B_\mu = B_{{\rm int},\mu} + B_{{\rm exc},\mu}$, as

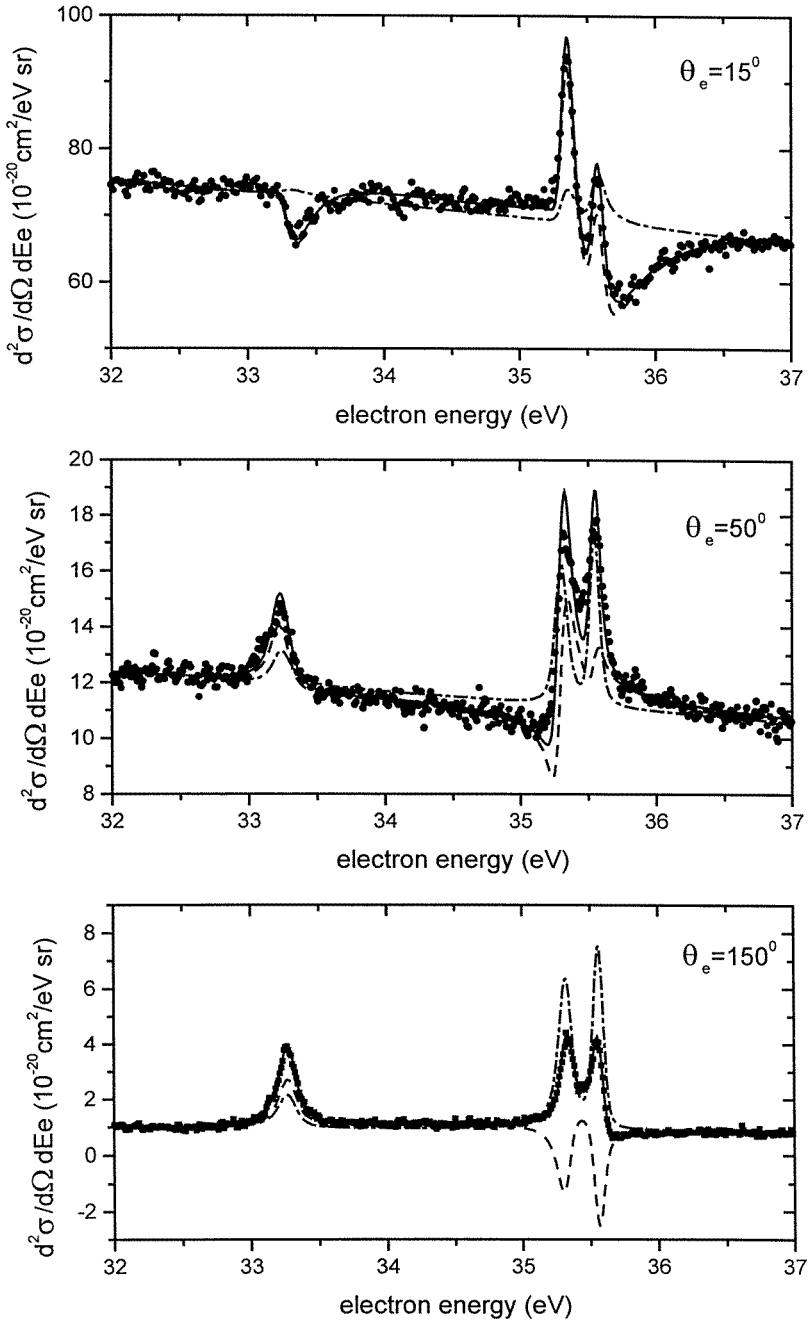

Figure 2. Experimental electron spectra in the region of the $(2s^2)^1S$, $(2p^2)^1D$ and $(2s2p)^1P$ resonances of helium excited by 100 keV proton impact, at the electron ejection angles of 15°, 50° and 130°. Energy resolution 68 meV. Experiment: full circles. Fitting results: full curve, spectra fitted with the full formula (24); broken curve, the contribution of interference with direct ionization; chain curve, resonance contribution.

indicated in section 2. In figure 2, we present experimental electron spectra in the region of the $(2s^2)^1S$, $(2p^2)^1D$ and $(2s2p)^1P$ resonances of helium excited by 100 keV proton impact fitted with the parametrization (24). As can be seen, interference of the direct and resonance transitions is almost completely responsible for the formation of the autoionization resonance profiles at small emission angles. As the emission angle increases, the interference contribution becomes smaller. Still, it remains comparable with the resonance contribution even for backward emission. A remarkable effect of the 'reversal' of the interference contribution in the transition from small to large emission angles should be attributed to the angular dependence of the amplitudes of direct ionization being combined with the angle-independent amplitudes of two-electron excitation.

It is clearly observable that the asymmetry of the resonance and interference contributions is small at large electron emission angles, where resonance profiles form as a result of enhancing (for the $(2s^2)^1S$ resonance) or compensating (for the $(2p^2)^1D$ and $(2s2p)^1P$ resonances) summation. That is why the intensity of the relatively 'weak' $(2s^2)^1S$ resonance can become nearly the same as the intensity of the 'strong' $(2s2p)^1P$ resonance for emission angles above 130°.

At large emission angles (figure 2(*c*)) the present experimental data clearly illustrate for the first time that the interference of direct and resonance channels can play an important role even when the resulting resonance shapes are nearly symmetrical. This indicates that in many collisional situations, when it is known that direct ionization coexists with the resonant one, calculations cannot neglect *a priori* the coupling of these two channels even when experimental electron spectra do not reveal any clear manifestation of interference patterns. Several examples can be found in earlier works which concerned the double excitation of helium at high-velocity proton impact (see references in I) as well as the transfer excitation in the $He^+ + He$ system (Itoh *et al* 1985, Gayet *et al* 1995); in the latter case the possibility of interference between transfer ionization and transfer excitation amplitudes has been recently incorporated into the calculations of Bachau *et al* (1997).

It is worth emphasizing that despite the fact that the three spectra shown in figure 2 are characterized by very different relative intensities and lineshapes, the fit which is shown was achieved by keeping the excitation cross section $\sigma_{\rm exc}^{LM}$ constant, independent of the emission angle as it must be. As just explained, the strong observed differences in the amplitudes of the observed resonances come from the interference terms which are strongly angle dependent.

7.2. Resonance parameters

The angular dependences of resonance parameters $A_{\rm int}$, $B_{\rm int}$ and $B_{\rm exc}$ for the $(2s^2)^1S$, $(2s2p)^1P$ and $(2p^2)^1D$ states are presented in figures 3–5, respectively.

There is no need to comment once again here on $A_{\rm int}$ since this parameter was already discussed in I and the experimental values obtained with the new fitting method are very near the values reported in I. On the other hand, the new fitting procedure also allows us to extract the absolute value and the angular behaviour of $B_{\rm int}$ which can be compared with those of $A_{\rm int}$. Extracting both parameters from electron spectra has also allowed us to derive the relative phase $\delta_\mu(E_{\rm i}, \theta_{\rm e})$ (see the definition given in equation (42); the discussion of this new quantity will be discussed later (see section 7.4)). It is found that both the magnitude and the angular dependence of parameters $A_{\rm int}$ and $B_{\rm int}$ are very similar; both oscillate strongly in the forward angle range and a slight dephasing is measured between them. The full calculation, employing second-order amplitudes as well as CIFS, is in qualitative agreement with experiment for all three resonances. The extrema of the calculated oscillations become nearer the experimental ones when including second-order terms. Second-Born calculations

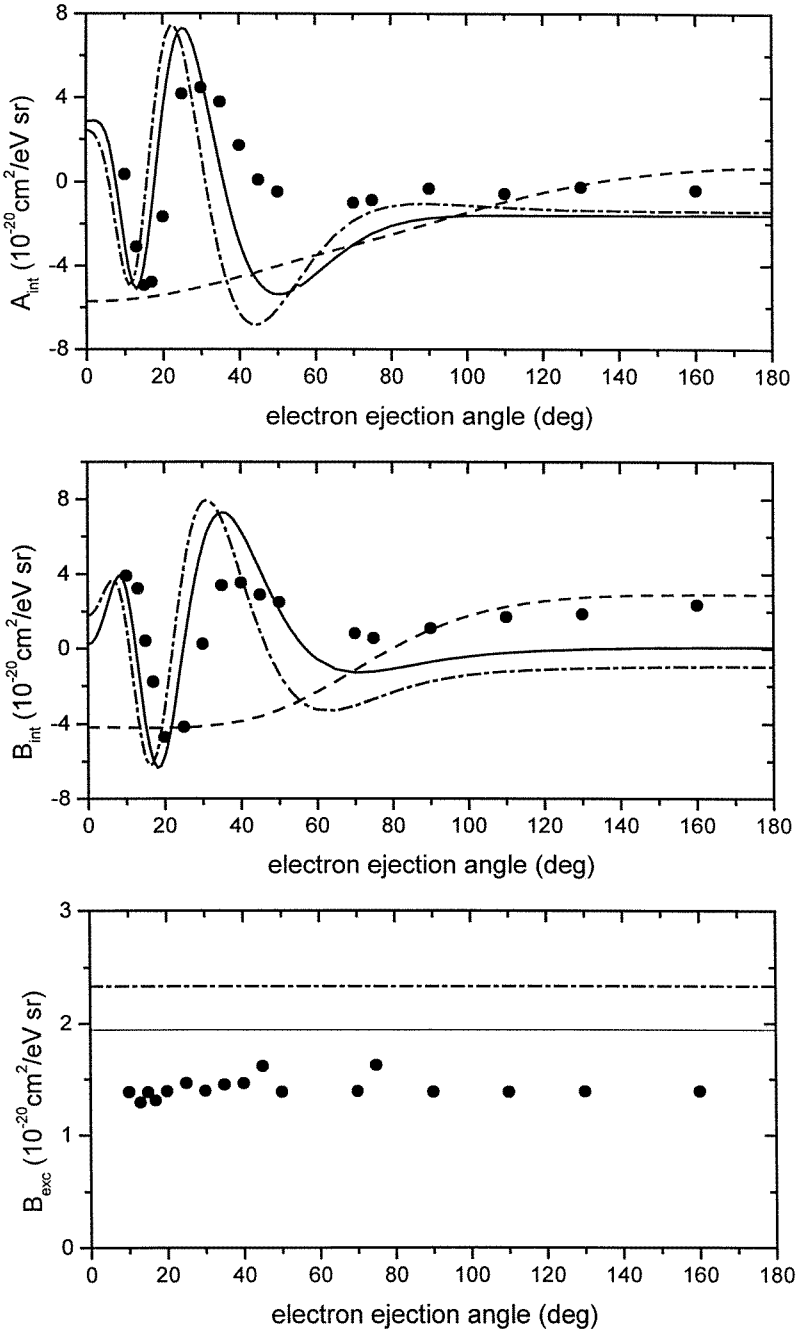

Figure 3. The angular dependence of resonance parameters $A_{\rm int}$, $B_{\rm int}$ and $B_{\rm exc}$ for the $(2s^2)^1$S state of helium excited by 100 keV proton impact. Experiment: full circles. Theory: full curve, full calculation; broken curve, calculation without CIFS; chain curve, calculations with CIFS and without the second-order terms in the amplitude of two-electron excitation. Parameter $B_{\rm exc}$ has been multiplied by $\sinh(\pi\xi)/(\pi\xi)$ to factor away the CIFS dependence.

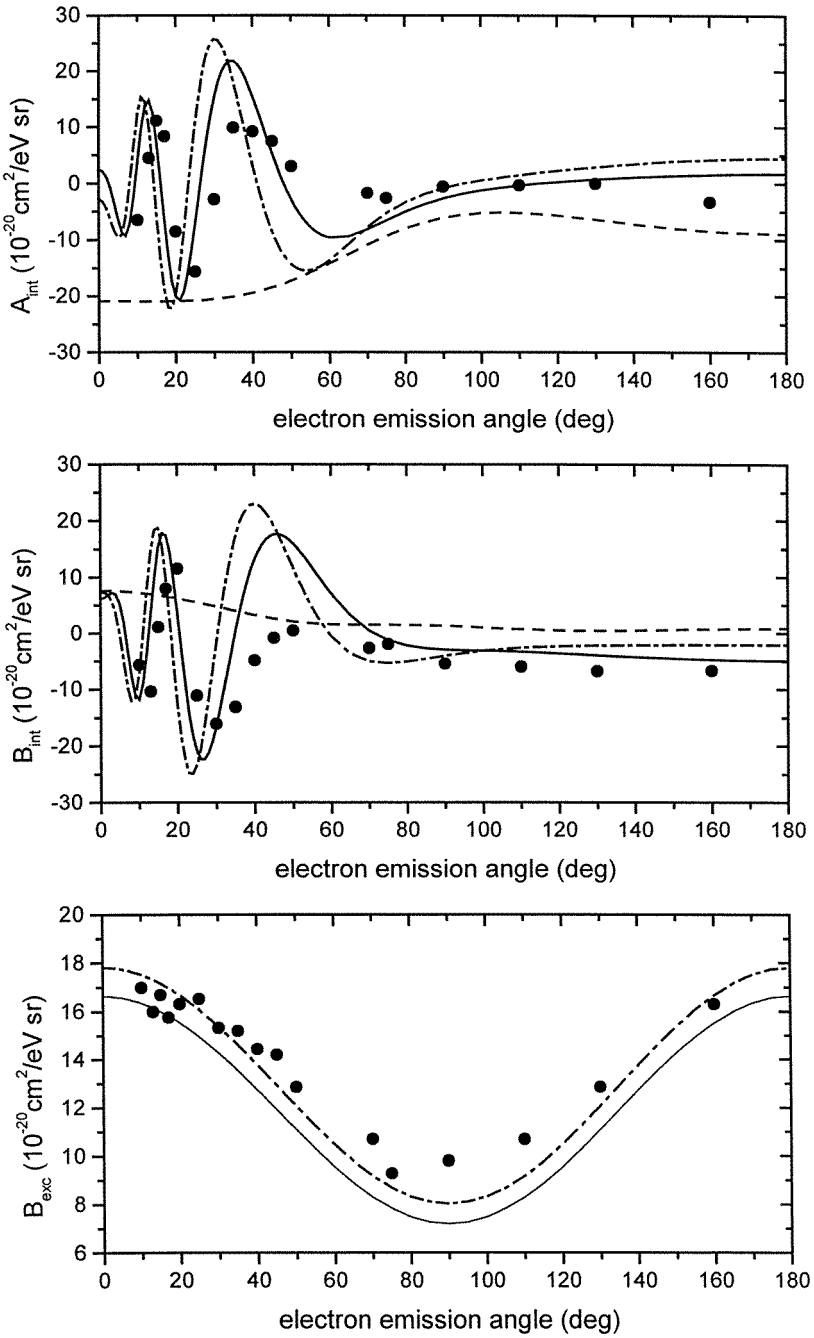

Figure 4. The same as figure 2 for the $(2s2p)^1P$ state of helium.

without CIFS fail to reflect the actual dependences at all, while first-Born calculations *with* CIFS reproduce much of the oscillatory structure observed at small ejection angles. Some discrepancy between experiment and theory is noted for the damping of the oscillations when

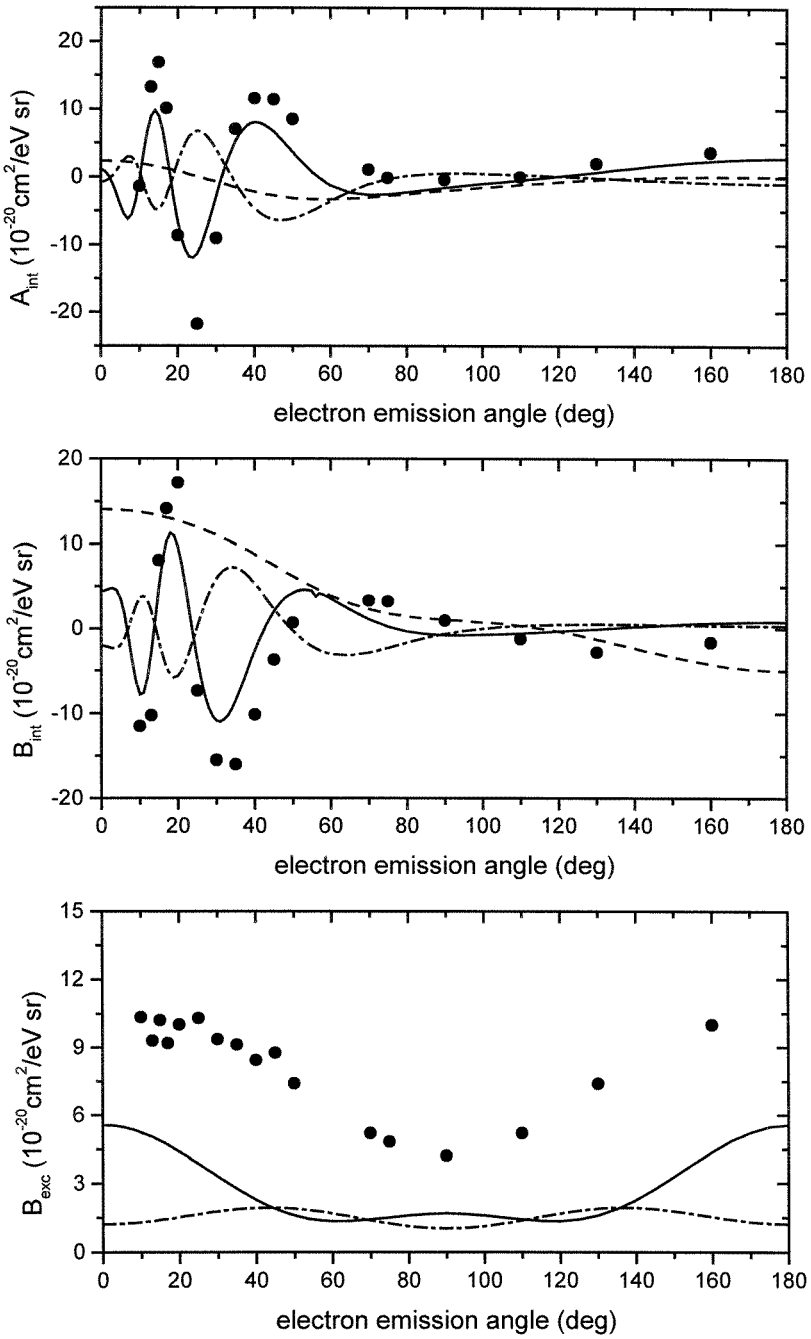

Figure 5. The same as figure 2 for the $(2p^2)^1$D state of helium.

the emission angle increases; the experimental one is stronger for the $(2s^2)^1$S and $(2s2p)^1$P resonances (30°–60°) angle range in figures 3 and 4, respectively (see also the related discussion in I).

The parameter $B_{\rm exc}$ has not been discussed before, and that is why we will pay more attention to it here. In figures 3–5, the reduced values of $B_{\rm exc}^{\rm red}$ are shown, obtained by multiplying $B_{\rm exc}$ by the factor $\sinh(\pi\xi)/(\pi\xi)$ (see equation (31)) which results in a cancelling of purely kinematic variations due to CIFS. According to equation (31), the resulting angular dependence must be determined by a sum of the squares of associated Legendre polynomials $P^2_{LM}(\cos\theta_{\rm e})$ weighted with partial cross sections $\sigma_{\rm exc}^{LM}$ of two-electron excitation of the target to the magnetic sublevel M.

For the $(2s^2)^1$S state, with $L = 0$, the reduced $B_{\rm exc}^{\rm red}$ does not depend on the angle, only the excitation cross section $\sigma_{\rm exc}^{00}$ being defined. The second-Born calculation is visibly closer to experiment than the analogous first-Born calculation. This implies that the electron density is rather diffused in this state, and hence must be significantly influenced by electron correlations. The polarization of the target by the projectile, partially accounted for in the second-order terms, is more pronounced in the interference coefficients, at large ejection angles, where one needs higher-order terms to describe experimental results.

The angular behaviour of the $(2s2p)^1$P state clearly reflects its multiplicity $L = 1$. A remarkable agreement between theory and experiment is observed for this resonance. From photoionization studies, it is well known that the coupling of the $(2s2p)^1$P state with the ionization continuum can be well described already in the lowest order, and correlations in the adjacent continuum are not significant for the decay process. However, the geometry of the state and its alignment by the projectile makes autoionization essentially coupled with the scattered projectile, which manifests itself in the discrepancies between theoretically calculated interference parameters $A_{\rm int}$ and $B_{\rm int}$ and the experimental data for forward ejection.

Calculation results for the $(2p^2)^1$D state indicate that there is a strong contribution of higher-order polarization effects in the target's excitation. The second-Born calculation is not enough to reproduce the observable behaviour of the excitation cross section. Experimental points seem to reveal an $L = 1$ rather than an $L = 2$ multiplicity, which might mean that the higher-order terms would sum up with peculiar phases, with the interference terms in the ionization cross section hence being very sensitive to the theoretical model used.

7.3. Cross sections of two-electron excitation

To explore the physical mechanisms beyond the process of two-electron excitation, we have performed a number of calculations, using a target excitation amplitude of the form

$$t_{\rm exc} = t_{\rm d1} + t_{\rm d2} + t_{\rm c1} \tag{45}$$

which includes the first-Born excitation amplitude $t_{\rm d1}$, the second-Born amplitude $t_{\rm d2}$ describing two-step transitions through singly excited states and the first-Born amplitude $t_{\rm c1}$ corresponding to the channel of excitation (specific for autoionizing states) via the adjacent continuum. The separation of the components of the full excitation amplitude is discussed in more detail in the appendix. The role of electron correlations in the target was investigated by comparing the results obtained with two sets of discrete-spectrum wavefunctions representing autoionizing states: one set was constructed from Slater-type wavefunctions within the configuration-interaction approximation (CI), and the other was calculated using the multiconfiguration Hartree–Fock method (MCHF). The total excitation cross section can be expressed through the sum of individual contributions and cross terms:

$$\sigma_{\rm exc} = \sum_i \sigma_i + \sum_{i<j} \sigma_{i,j} \tag{46}$$

with

$$\sigma_i = (2\pi)^4 m_\mathrm{p}^2 \frac{K_\mathrm{f}}{K_\mathrm{i}} \sum_{M=-L}^{L} \int |t_i|^2 \, \mathrm{d}\Omega_\mathrm{f} \tag{47}$$

and

$$\sigma_{ij} = (2\pi)^4 m_\mathrm{p}^2 \frac{K_\mathrm{f}}{K_\mathrm{i}} \sum_{M=-L}^{L} \int 2\,\mathrm{Re}(t_i t_j^*) \, \mathrm{d}\Omega_\mathrm{f} \tag{48}$$

where $i, j = \mathrm{d1}, \mathrm{d2}, \mathrm{c1}$.

Table 1. Cross section (in units of 10^{-20} cm^2) for two-electron excitation of the autoionizing $(2s^2)^1$S, $(2s2p)^1$P and $(2p^2)^1$D states of helium excited by 100 keV proton impact.

	$(2s^2)^1$S		$(2s2p)^1$P		$(2p^2)^1$D	
	CI	MCHF	CI	MCHF	CI	MCHF
σ_{d1}	8.62	4.54	7.05	5.99	1.40	0.32
σ_{d2}	2.54	2.35	5.22	5.06	7.97	7.65
σ_{c1}	1.99	1.97	2.51	2.92	2.53	2.08
$\sigma_{\mathrm{d1,d2}}$	0.72	0.55	0.90	0.74	1.01	0.46
$\sigma_{\mathrm{d1,c1}}$	−0.93	0.66	0.65	1.97	−1.16	−0.17
$\sigma_{\mathrm{d2,c1}}$	−4.29	−4.10	−6.51	−6.72	−8.11	−7.33
σ_{th}	8.64	5.97	9.81	9.96	3.64	3.00
σ_{exp}	3.40		8.80		9.00	
$\sigma_{\mathrm{exp,Schulz}}$	9.70		21.0[a]			

[a] The sum of (^{1}P + ^{1}D).

The results for the total excitation cross sections and their components are presented in table 1 along with our experimental data. The figures differ a little from those presented in Moretto-Capelle *et al* (1997), since more accurate summation algorithms have been used here. In table 1 we also show experimental data of Schulz *et al* (1995) derived by an analysis of the resonance yield in energy loss spectra as a function of the scattering angle. Owing to the low-energy resolution the $(2p^2)^1$D and $(2s2p)^1$P resonances were unresolved in Schulz *et al* (1995). Therefore, the sum of cross sections for these states is displayed which is in good agreement with our experimental results. For $(2s^2)^1$S there is a difference between the two experimental cross sections, but the experimental error is remarkable for energy loss measurements (9.7 ± 7.0 in units of 10^{-20} cm^2).

While the theoretical estimate of the total excitation cross section for the $(2s2p)^1$P resonance agrees satisfactorily with experiment, the cross section for the $(2s^2)^1$S state is overestimated and for the $(2p^2)^1$D state is significantly underestimated. Such a discrepancy is due to the higher-order contributions not included in the model. As noted in the previous section, it can be seen that σ_{d1} plays an important role in the excitation of the $(2s^2)^1$S and $(2s2p)^1$P resonances, but not for that of $(2p^2)^1$D (see also I).

Among the qualitative conclusions one could draw on the basis of table 1, we would point to a highly destructive (for a positive projectile) interference between the two-step mechanism and the continuum-mediated excitation, as indicated by the $\sigma_{\mathrm{d2,c1}}$ cross term. For all the resonances considered, σ_{d2} prevails over σ_{c1}, that is, the amplitude t_{d2} is greater than t_{c1} in absolute value; however, the continuum component of the autoionizing state, as defined by equation (A33), seems to screen the effect of the projectile and hence damps the two-step process. The two-step t_{d2} and continuum-mediated t_{c1} channels proved to be almost insensitive to the quality of the

orbitals. In contrast, the cross section σ_{d1} (and its interference with the other channels) requires taking account of the correlation effects accurately.

We can see that two-electron excitation is a complex process involving many interfering mechanisms, and it would be an oversimplification to identify an autoionizing state with a doubly excited discrete-spectrum state in the target, retaining only the amplitudes t_{d1} and t_{d2} in (45). Most theoreticians stick to this approximation, since properly accounting for other mechanisms requires much analytical and computational effort. However, as our analysis shows, one can obtain only random agreement with experiment without a correct description of the excitation processes involved. Thus, the close reproduction of our experimental data (Moretto-Capelle *et al* 1997) by Bodea *et al* (1998), who did not account for the embedding of autoionizing states in the continuum at all, could serve as an example of how good agreement with experiment may indicate incompleteness of the theoretical model rather than its adequacy.

Table 2. Sublevel populations ($M = 0, \pm1, \pm2$) in %.

	$(2s2p)^1P$			$(2p^2)^1D$		
	CI	MCHF	Expt	CI	MCHF	Expt
d1	56 44	59 41		32 55 13	18 58 24	
d2	71 29	71 29		41 48 11	41 48 11	
c1	49 51	49 51		20 59 21	19 59 22	
Total	53 47	54 46	51 49	53 40 7	54 38 8	32 57 11

Table 2 presents the calculated values for the population of magnetic sublevels of the $(2s2p)^1P$ and $(2p^2)^1D$ states, both total and by excitation channel, compared with experiment. Generally, the population distributions appear to be less sensitive to the choice of the orbitals (cf CI or MCHF results). The first-order mechanism is rather close to experiment; this is particularly remarkable for the d_1 CI calculations which reproduce very well the experimental sublevel populations even for the $(2p^2)^1D$ state. This agreement seems fortuitous since a poor agreement was already noted with the Born I calculations for A_{int} and B_{int} (figure 4) and for the total excitation cross section (table 1). In the theoretical model used, two-step excitation overpopulates the sublevel with $M = 0$, which indicates the necessity of accounting for multipole polarization of the target, especially in the case of the $(2p^2)^1D$ state.

7.4. Relative phase

The dimensionless phase parameter $\delta_\mu(E_i, \theta_e)$ defined by equation (42) could be used to study resonance profile formation. In the triply differential cross section the relative phase $\delta_\mu(E_i, \theta_e, \theta_f)$ has a clear meaning of a relative phase between the direct and resonant ionization amplitudes (Godunov *et al* 1990). On the other hand, the relative phase $\delta_\mu(E_i, \theta_e)$ which can be defined from the doubly differential cross section is not straightforward since the interference terms in A_{int} and B_{int} result from an integration over the scattering angle.

Theoretical and experimental angular dependences of $\delta_\mu(E_i, \theta_e)$ for the $(2s^2)^1S$, $(2s2p)^1P$ and $(2p^2)^1D$ resonances are given in figure 6. The remarkable fact is that, despite the discrepancies with the experiment in the other resonance parameters, excitation cross sections and magnetic sublevel population, theoretical phases are in good agreement with experimental data. This might mean that parametrization (43) is fundamental enough, reflecting some essential features of the ionization process. In the back hemisphere, the calculation without CIFS already provides a reasonable estimate of the phase; however, the account for post-collision kinematics is important to describe the behaviour of the phase for ejection angles

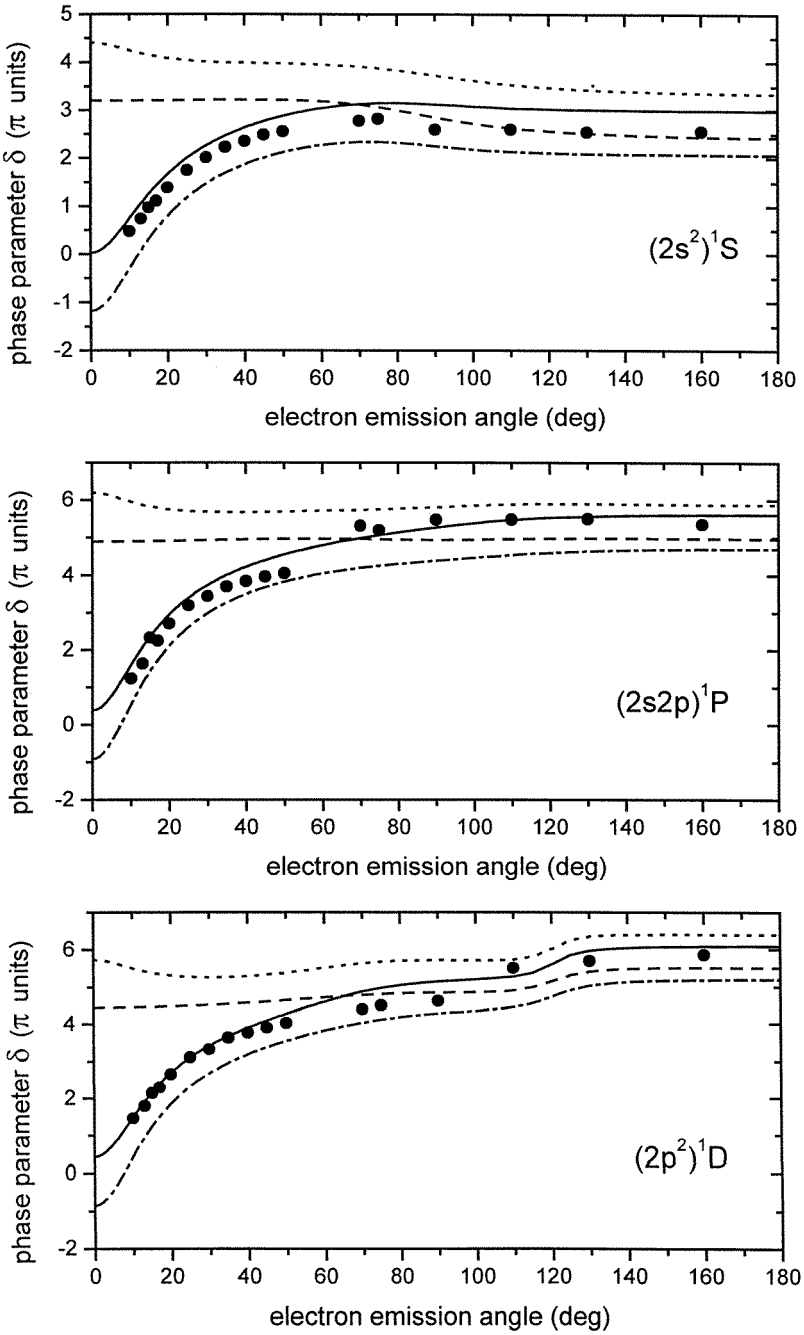

Figure 6. Relative phase δ for the autoionizing $(2s^2)^1S$, $(2s2p)^1P$ and $(2p^2)^1D$ states of helium excited by 100 keV proton impact. Experiment: full circles. Theory: full curve, the full calculation; chain curve, calculation CIFS included in the resonance channel only; broken curve, calculation with CIFS in the direct ionization channel only; dotted curve, calculation without CIFS in the second Born approximation.

below 60°. Including CIFS in the resonance terms of the total ionization amplitude would qualitatively reproduce the observed phases, though it is necessary to include CIFS in direct ionization amplitudes too, to attain a quantitative agreement; still, accounting for CIFS in direct ionization alone cannot reproduce the observable behaviour.

The angular dependence $\delta_\mu(E_\mathrm{i}, \theta_\mathrm{e})$ characterizes the dependence of the resonance form on collision kinematics. The similarity of that dependence for the resonances of quite different symmetry and structure indicates that the major contribution to the phase comes from the interactions in the asymptotic region far from the residual ion, and the structure of the autoionizing state and its formation processes cannot be clearly reflected in that quantity. The form of the dependence suggests that there is a universal kinematic component that can be excluded from the phase (42) to obtain a different parameter that would provide a more sensitive test of the interplay of various atomic processes (Godunov *et al* 1990).

8. Conclusions

We have addressed the problem of extracting information about the cross sections of AIS excitation from experimental data on heavy particle collisions with atoms. The principal results may be summarized as follows.

(a) AIS can be considered as true atomic states, albeit of a particular sort. Using a specially designed technique, one can measure the energies, widths and excitation probabilities of AIS regardless of the channels of their subsequent decay.

(b) Separation of AIS excitation from direct ionization and decay can only be performed under the conditions of the strong influence of a rapidly varying external field on the AIS decay process, resulting in deviations of the resonance shape from Fano/Shore profiles, which can be described by additional profile parameters. Fitting experimental data with the thus obtained parametric formulae, one can determine excitation cross sections for individual magnetic sublevels of AIS.

(c) The general approach suggested here has been applied to the reaction of single ionization of helium by a heavy charged projectile, where the explicit analytical expressions for the kinematic factor could be obtained in the eikonal limit. The profile parameters for the $(2s^2)^1S$, $(2p^2)^1D$ and $(2s2p)^1P$ resonances excited by 100 keV proton impact have been calculated theoretically, and the cross sections of two-electron excitation and populations of the magnetic sublevels of the $(2p^2)^1D$ and $(2s2p)^1P$ states have been estimated theoretically.

(d) A new parametric formula has been used to process experimental high-resolution spectra of electron emission at different angles, which has allowed us to extract theoretically introduced quantities from the experimental data. The results for profile parameters, excitation cross sections, sublevel populations and relative phases have been compared with experiment, and the underlying physical mechanisms have been discussed. The overall agreement with experiment supports the applicability of the approach suggested.

Acknowledgments

We would like to thank Professor J McGuire for useful discussions. One of the authors (ALG) was supported by the Division of Chemical Sciences, Office of Basic Energy Science, Office of Energy Research, US Department of Energy.

Appendix. Resonant ionization in the diagonalization approach

The diagonalization method was originally developed in a differential formulation by Balashov *et al* (1968). It was subsequently complemented by an integral formalism by Ivanov and Senashenko (1983) and then Howat *et al* (1978). The equivalence of the two forms has been demonstrated by Ivanov (1989) for a wide class of physical problems. Both differential (Godunov *et al* 1989) and integral formalisms have been developed for our calculations, and we could use both, for reasons of convenience. An integral approach will be used here, to make the presentation of results more concise and transparent.

The helium atom and a structureless projectile form a four-particle system, which can be described by the Hamiltonian in the simplified Jacobi coordinates

$$\widehat{H} = \sum_{i=1}^{2}\left(-\frac{1}{2\mu_{\mathrm{t}}}\nabla_{r_i}^2 - \frac{Z_{\mathrm{t}}}{r_i}\right) + \frac{1}{|\boldsymbol{r}_1-\boldsymbol{r}_2|} - \frac{1}{2\mu_{\mathrm{p}}}\nabla_{\boldsymbol{R}}^2 - \sum_{i=1}^{2}\frac{Z_{\mathrm{p}}}{|\boldsymbol{r}_i-\boldsymbol{R}|} + \frac{Z_{\mathrm{t}}Z_{\mathrm{p}}}{R}$$
$$= \widehat{h}_1 + \widehat{h}_2 + \widehat{V}_{12} + \widehat{h}_{\mathrm{p}} + \widehat{V}_{\mathrm{p}} = \widehat{H}_{\mathrm{t}} + \widehat{h}_{\mathrm{p}} + \widehat{V}_{\mathrm{p}}. \tag{A1}$$

The eigenfunctions of this Hamiltonian depend on the quantum numbers referring to both the target electrons and the projectile. We denote the momentum of the projectile by $\boldsymbol{K}$, the total energy including the kinematic energy of the projectile by E and all the other discrete and continuous parameters (e.g. the electron emission angle) by a.

The final state of ionization must satisfy the Schrödinger equation

$$(E - \widehat{H})|a\boldsymbol{K}E) = 0. \tag{A2}$$

Following the traditional procedure of Fano (1961), we seek the solution of (A2) in the form

$$|a\boldsymbol{K}E) = \sum_{\lambda}\int \mathrm{d}\widetilde{\boldsymbol{K}}\,|\lambda\widetilde{\boldsymbol{K}}\rangle\Lambda_{\lambda}(\widetilde{\boldsymbol{K}}; a\boldsymbol{K}E) + \sum_{b}\int \mathrm{d}\widetilde{E}\int \mathrm{d}\widetilde{\boldsymbol{K}}\,|b\widetilde{\boldsymbol{K}}\widetilde{E}\rangle C_b(\widetilde{\boldsymbol{K}}\widetilde{E}; a\boldsymbol{K}E). \tag{A3}$$

States $|\lambda\widetilde{\boldsymbol{K}}\rangle$ include no outgoing waves for target electrons and represent the states with no free electrons (*closed channels*); states $|b\widetilde{\boldsymbol{K}}\widetilde{E}\rangle$ imply one outgoing wave for an atomic electron and represent the states of a singly ionized target interacting with a scattered projectile (*open channels*). We neglect double-ionization states in expansion (A3), as well as the states related to the formation of a quasi-molecule. Since the basis sets for both closed and open channels can be chosen arbitrarily, we fix the vector sets by using the conditions

$$\langle\lambda\boldsymbol{K}'|\widehat{H} - E|\nu\boldsymbol{K}''\rangle = (E_\lambda(\boldsymbol{K}) - E)\delta_{\lambda\nu}\delta(\boldsymbol{K}'-\boldsymbol{K}'') + V_{\lambda\nu}(\boldsymbol{K}', \boldsymbol{K}''; E) \tag{A4}$$

$$\langle b\boldsymbol{K}'E'|\widehat{H} - E|c\boldsymbol{K}''E''\rangle = (E'-E)\delta_{bc}\delta(\boldsymbol{K}'-\boldsymbol{K}'')\delta(E'-E'') \tag{A5}$$

$$\langle\lambda\boldsymbol{K}'|\widehat{H} - E|b\boldsymbol{K}''E''\rangle = V_{\lambda b}(\boldsymbol{K}', \boldsymbol{K}''E''; E) \tag{A6}$$

$$\langle b\boldsymbol{K}'E'|\widehat{H} - E|\lambda\boldsymbol{K}''\rangle = V_{b\lambda}(\boldsymbol{K}'E', \boldsymbol{K}''; E) = V^*_{\lambda b}(\boldsymbol{K}'', \boldsymbol{K}'E'; E). \tag{A7}$$

In general, we do not demand orthogonality of open and closed channels, and the only restriction on the basis vectors in the closed-channels subspace is the condition of 'weak' orthonormality:

$$\langle\lambda\boldsymbol{K}'|\nu\boldsymbol{K}''\rangle = \delta_{\lambda\nu}\delta(\boldsymbol{K}'-\boldsymbol{K}'') + O_{\lambda\nu}(\boldsymbol{K}', \boldsymbol{K}''). \tag{A8}$$

As has been demonstrated by Ramaker (1971) and Ramaker and Schraeder (1974), normalization and orthogonality can be entirely abandoned for the basis sets, though the physical side of the theory becomes much less transparent in that case.

Typically, a finite number of closed-channel basis vectors are selected to be orthonormalized and diagonalize $\widehat{H}_{\rm t}$, so that

$$E_\lambda(\boldsymbol{K}) = E_\lambda + \frac{K^2}{2\mu_{\rm p}} \qquad \text{and} \qquad V_{\lambda\nu}(\boldsymbol{K}', \boldsymbol{K}'') = \langle \lambda \boldsymbol{K}' | \widehat{V}_{\rm p} | \nu \boldsymbol{K}'' \rangle. \tag{A9}$$

This is known as the restricted CI procedure (Fano 1961). However, there may be other choices, and, in general, the dependence of $E_\lambda(\boldsymbol{K})$ on $\boldsymbol{K}$ may be not separable from the dependence on λ.

Constructing an open-channel basis satisfying condition (A5) is known as prediagonalization (Fano and Prats 1973). For a final state containing only one free particle, prediagonalization can be reduced to the solution of a set of integral equations; with several free particles in the final state, prediagonalization is not trivial and requires additional assumptions, some of which will be discussed later.

Projecting Schrödinger equation (A2) onto either a closed channel $\langle \lambda \boldsymbol{K}'|$ or an open channel $\langle b \boldsymbol{K}' E'|$, one obtains

$$(E - E_\lambda(\boldsymbol{K}'))\Lambda_\lambda(\boldsymbol{K}'; a\boldsymbol{K}E) - \sum_\nu \int \mathrm{d}\widetilde{\boldsymbol{K}}\, V_{\lambda\nu}(\boldsymbol{K}', \widetilde{\boldsymbol{K}}; E)\Lambda_\nu(\widetilde{\boldsymbol{K}}; a\boldsymbol{K}E)$$
$$- \sum_b \int \mathrm{d}\widetilde{E} \int \mathrm{d}\widetilde{\boldsymbol{K}}\, V_{\lambda b}(\boldsymbol{K}', \widetilde{\boldsymbol{K}}\widetilde{E}; E) C_b(\widetilde{\boldsymbol{K}}\widetilde{E}; a\boldsymbol{K}E) = 0 \tag{A10}$$

$$(E - E')C_b(\boldsymbol{K}'; a\boldsymbol{K}E) - \sum_\nu \int \mathrm{d}\widetilde{\boldsymbol{K}}\, V_{b\nu}(\boldsymbol{K}'E', \widetilde{\boldsymbol{K}}; E)\Lambda_\nu(\widetilde{\boldsymbol{K}}; a\boldsymbol{K}E) = 0. \tag{A11}$$

Using the techniques of Howat *et al* (1978), one can obtain from (A11) and the open-channel asymptote that

$$C_b(\boldsymbol{K}'; a\boldsymbol{K}E) = \delta_{ba}\delta(\boldsymbol{K}' - \boldsymbol{K})\delta(E' - E)$$
$$+ \sum_\nu \int \mathrm{d}\widetilde{\boldsymbol{K}}\, V_{b\nu}(\boldsymbol{K}'E', \widetilde{\boldsymbol{K}}; E)\Lambda_\nu(\widetilde{\boldsymbol{K}}; a\boldsymbol{K}E) \frac{1}{E - E' \pm \mathrm{i}0} \tag{A12}$$

which, after substitution into equation (A10), gives

$$\sum_\nu \int \mathrm{d}\boldsymbol{K}'' \left\{ (E - E_\lambda(\boldsymbol{K}'))\delta_{\lambda\nu}\delta(\boldsymbol{K}' - \boldsymbol{K}'') - \Delta_{\lambda\nu}(\boldsymbol{K}', \boldsymbol{K}''; E) \right\} \Lambda_\nu(\boldsymbol{K}''; a\boldsymbol{K}E)$$
$$= V_{\lambda a}(\boldsymbol{K}', \boldsymbol{K}E; E) \tag{A13}$$

with

$$\Delta_{\lambda\nu}(\boldsymbol{K}', \boldsymbol{K}''; E) = V_{\lambda\nu}(\boldsymbol{K}', \boldsymbol{K}''; E)$$
$$+ \sum_b \int \mathrm{d}\widetilde{\boldsymbol{K}} \int \frac{\mathrm{d}\widetilde{E}}{E - \widetilde{E} \pm \mathrm{i}0} V_{\lambda b}(\boldsymbol{K}', \widetilde{\boldsymbol{K}}\widetilde{E}; E) V_{b\nu}(\widetilde{\boldsymbol{K}}\widetilde{E}, \boldsymbol{K}''; E). \tag{A14}$$

With $\Lambda_\nu(\boldsymbol{K}'; a\boldsymbol{K}E)$ obtained from (A13), one can construct a complete final-state vector as

$$|a\boldsymbol{K}E) = |a\boldsymbol{K}E\rangle + \sum_\lambda \int \mathrm{d}\boldsymbol{K}'\, |(\lambda E)\boldsymbol{K}'\rangle \Lambda_\lambda(\boldsymbol{K}'; a\boldsymbol{K}E) \tag{A15}$$

where we have introduced 'modified' closed-channel states (Fano 1961) as

$$|(\lambda E)\boldsymbol{K}'\rangle = |\lambda \boldsymbol{K}'\rangle + \sum_b \int \mathrm{d}\widetilde{\boldsymbol{K}} \int \frac{\mathrm{d}\widetilde{E}}{E - \widetilde{E} \pm \mathrm{i}0} |b\widetilde{\boldsymbol{K}}\widetilde{E}\rangle V_{b\lambda}(\widetilde{\boldsymbol{K}}\widetilde{E}, \boldsymbol{K}'; E). \tag{A16}$$

It is these 'modified' states that determine the process of multiple excitation of the target by the projectile. It should be noted that, in general, $V_{b\lambda}$ contains contributions from the operator $\widehat{V}_{\rm p}$, and hence the second term in (A16) incorporates the polarization mechanism of the excitation of an autoionizing state via an adjacent continuum.

Coefficients $\Lambda_\nu(\boldsymbol{K}'; a\boldsymbol{K}E)$ contain resonant denominators responsible for autoionization resonances in cross sections, as well as the amplitudes of autoionization $V_{\lambda a}(\boldsymbol{K}', \boldsymbol{K}E; E)$ and the amplitudes of transition between different autoionization states $\Delta_{\lambda\nu}(\boldsymbol{K}', \boldsymbol{K}''; E)$ containing both residual interaction $V_{\lambda\nu}(\boldsymbol{K}', \boldsymbol{K}''; E)$ and transitions through the adjacent continuum described by the integral term in (A14). If a CI basis has been chosen for the closed-channel subspace, $V_{\lambda\nu}$ will represent the interaction with the projectile only; the influence of relatively slow charged projectiles on autoionization could be studied in this way. An alternative possibility is to use a completely prediagonalized basis for closed channels, with $V_{\lambda\nu} = 0$. This would mean considering autoionizing states polarized by the projectile.

As the coupled integral equation (A13) is too complex to solve exactly, it is approximate solutions that are of primary importance for a theoretical model. Calculations presented in the present paper have been performed using a 'strong diagonalization' approach, setting

$$\Delta_{\lambda\nu}(\boldsymbol{K}', \boldsymbol{K}''; E) \approx \Delta_{\lambda\lambda}(\boldsymbol{K}', \boldsymbol{K}'; E)\delta_{\lambda\nu}\delta(\boldsymbol{K}' - \boldsymbol{K}'') \tag{A17}$$

so that

$$\Lambda_\lambda(\boldsymbol{K}'; a\boldsymbol{K}E) = \frac{V_{\lambda a}(\boldsymbol{K}', \boldsymbol{K}E; E)}{E - E_\lambda(\boldsymbol{K}') - \Delta_{\lambda\lambda}(\boldsymbol{K}', \boldsymbol{K}'; E)}. \tag{A18}$$

The real and imaginary parts of $\Delta_{\lambda\lambda}(\boldsymbol{K}', \boldsymbol{K}'; E)$ give the resonance shift and width

$$\Delta E_\lambda(\boldsymbol{K}'E) = V_{\lambda\lambda}(\boldsymbol{K}', \boldsymbol{K}'; E) + \sum_b \int \mathrm{d}\widetilde{\boldsymbol{K}} \int \frac{\mathrm{d}\widetilde{E}}{E - \widetilde{E} \pm \mathrm{i}0} \left|V_{\lambda b}(\boldsymbol{K}', \widetilde{\boldsymbol{K}}\widetilde{E}; E)\right|^2. \tag{A19}$$

$$\Gamma_\lambda(\boldsymbol{K}'E) = 2\pi \sum_b \int \mathrm{d}\widetilde{\boldsymbol{K}} \left|V_{\lambda b}(\boldsymbol{K}', \widetilde{\boldsymbol{K}}E; E)\right|^2. \tag{A20}$$

In general, an autoionization resonance becomes shifted and broadened due to both interaction with the projectile and virtual transitions into the continuum. It should be noted that, in the general case, resonance position

$$E_\lambda(\boldsymbol{K}'E) = E_\lambda(\boldsymbol{K}') - \frac{(K')^2}{2\mu_{\rm p}} + \Delta E_\lambda(\boldsymbol{K}'E) \tag{A21}$$

and width $\Gamma_\lambda(\boldsymbol{K}'E)$ are both functions of projectile momentum and final-state energy. It is under certain additional assumptions only that one could speak of AIS position and width as atomic constants.

The amplitude of transition from an initial state (target in the ground state, incoming projectile with momentum $\boldsymbol{K}_0$) to a final state $|a\boldsymbol{K}E)$ can be calculated as

$$\begin{aligned} t(a\boldsymbol{K}E|\boldsymbol{K}_0) &= (a\boldsymbol{K}E|\widehat{V}_{\rm p}|\boldsymbol{K}_0) \\ &= t_{\rm dir}(a\boldsymbol{K}E|\boldsymbol{K}_0) + \sum_\lambda \int \mathrm{d}\boldsymbol{K}' \frac{t_{{\rm res},\lambda}(a\boldsymbol{K}E, \boldsymbol{K}'|\boldsymbol{K}_0)}{E - E_\lambda(\boldsymbol{K}') - \Delta E_\lambda(\boldsymbol{K}'E) + \frac{1}{2}\mathrm{i}\Gamma_\lambda(\boldsymbol{K}'E)} \end{aligned} \tag{A22}$$

with

$$t_{\rm dir}(a\boldsymbol{K}E|\boldsymbol{K}_0) = \langle a\boldsymbol{K}E|\widehat{V}_{\rm p}|\boldsymbol{K}_0) \tag{A23}$$

$$\begin{aligned} t_{{\rm res},\lambda}(a\boldsymbol{K}E, \boldsymbol{K}'|\boldsymbol{K}_0) &= \langle a\boldsymbol{K}E|\widehat{H} - E|\lambda\boldsymbol{K}'\rangle\langle(\lambda E)\boldsymbol{K}'|\widehat{V}_{\rm p}|\boldsymbol{K}_0) \\ &= t_{{\rm dec},\lambda}(a\boldsymbol{K}E, \boldsymbol{K}')t_{{\rm exc},\lambda}(\boldsymbol{K}'E|\boldsymbol{K}_0). \end{aligned} \tag{A24}$$

Since matrix elements (A6) and (A7) are calculated with the full Hamiltonian $\widehat{H}$, amplitudes (A23) and (A24) include higher-order terms in $\widehat{V}_{\rm p}$ as well. From (A20) and (A24) one can see that

$$\Gamma_\lambda(\boldsymbol{K}'E) = 2\pi \sum_b \int \mathrm{d}\widetilde{\boldsymbol{K}}\ \left|t_{\mathrm{dec},\lambda}(b\widetilde{\boldsymbol{K}}E, \boldsymbol{K}')\right|^2. \tag{A25}$$

We will call $t_{\mathrm{exc},\lambda}$ the amplitude of the excitation of autoionization state λ; the quantity

$$\sigma_{\mathrm{exc},\lambda} = C\left|t_{\mathrm{exc},\lambda}(\boldsymbol{K}'E, \boldsymbol{K}_0)\right|^2 \tag{A26}$$

with an appropriate factor C, will be called the cross section of AIS excitation; it is directly related to experimentally observable quantities, as shown in this paper.

For three free particles in the final state, open-channel prediagonalization is quite non-trivial, and one has to make additional assumptions about the structure of continuum wavefunctions. For fast enough projectiles, we can neglect polarization of autoionizing states and adjacent continua by the projectile and describe the projectile's motion with a plane-wave state $|\overline{\boldsymbol{K}}\rangle$, expanding prediagonalized states $|a\boldsymbol{K}E\rangle$ into a sum of product states $|pE_{\rm t}\rangle|\overline{\boldsymbol{K}}\rangle$, with $E_{\rm t} = E - \overline{K}^2/2\mu_{\rm p}$

$$|a\boldsymbol{K}E\rangle = \sum_p \int \mathrm{d}\overline{\boldsymbol{K}}\,|pE_{\rm t}\rangle|\overline{\boldsymbol{K}}\rangle\zeta(p\overline{\boldsymbol{K}}; a\boldsymbol{K}E). \tag{A27}$$

Using (A27) and the completeness conditions

$$\sum_a \int \mathrm{d}\boldsymbol{K}\,\zeta(p\overline{\boldsymbol{K}}; a\boldsymbol{K}E)\zeta^*(p'\overline{\boldsymbol{K}}'; a\boldsymbol{K}E) = \delta_{pp'}\delta(\overline{\boldsymbol{K}} - \overline{\boldsymbol{K}}') \tag{A28}$$

$$\int \mathrm{d}\overline{\boldsymbol{K}}\,|\overline{\boldsymbol{K}}\rangle\langle\overline{\boldsymbol{K}}| = 1 \tag{A29}$$

one obtains

$$\sum_b \int \mathrm{d}\widetilde{\boldsymbol{K}} \int \frac{\mathrm{d}\widetilde{E}}{E - \widetilde{E} \pm \mathrm{i}0}|b\widetilde{\boldsymbol{K}}\widetilde{E}\rangle\langle b\widetilde{\boldsymbol{K}}\widetilde{E}| = \sum_p \int \frac{\mathrm{d}\widetilde{E}_{\rm t}}{E_{\rm t} - \widetilde{E}_{\rm t} \pm \mathrm{i}0}|p\widetilde{E}_{\rm t}\rangle\langle p\widetilde{E}_{\rm t}|. \tag{A30}$$

Formula (A30) allows one to replace summations over the compound states target + projectile with summations over target states only, where projectile-induced polarization is not important; such a replacement significantly simplifies calculations. Still, final state vectors in AIS decay amplitudes $t_{\mathrm{dec},\lambda}$ and direct ionization amplitudes $t_{\rm dir}$ cannot be simplified in that way, and one has to account for essentially three-particle kinematics (Godunov *et al* 1989).

Splitting amplitudes $V_{\lambda b}$ into two parts,

$$\langle\lambda\boldsymbol{K}'|\widehat{H} - E|b\boldsymbol{K}''E''\rangle = \langle\lambda\boldsymbol{K}'|\widehat{H}_{\rm t} + \widehat{h}_{\rm p} - E|b\boldsymbol{K}''E''\rangle + \langle\lambda\boldsymbol{K}'|\widehat{V}_{\rm p}|b\boldsymbol{K}''E''\rangle \tag{A31}$$

and using substitution (A30), we can rewrite

$$\begin{aligned} t_{\mathrm{exc},\lambda}(\boldsymbol{K}'E|\boldsymbol{K}_0) &= \langle\lambda\boldsymbol{K}'|\widehat{V}_{\rm p}|\boldsymbol{K}_0\rangle \\ &\quad + \sum_b \int \mathrm{d}\widetilde{\boldsymbol{K}} \int \frac{\mathrm{d}\widetilde{E}}{E - \widetilde{E} \mp \mathrm{i}0}\, V_{\lambda b}(\boldsymbol{K}', \widetilde{\boldsymbol{K}}\widetilde{E}; E)\langle b\widetilde{\boldsymbol{K}}\widetilde{E}|\widehat{V}_{\rm p}|\boldsymbol{K}_0\rangle \\ &= \langle\lambda\boldsymbol{K}'|\widehat{V}_{\rm p}|\boldsymbol{K}_0\rangle + \sum_b \int \mathrm{d}\widetilde{\boldsymbol{K}} \int \frac{\mathrm{d}\widetilde{E}}{E - \widetilde{E} \mp \mathrm{i}0}\,\langle\lambda\boldsymbol{K}'|\widehat{V}_{\rm p}|b\widetilde{\boldsymbol{K}}\widetilde{E}\rangle\langle b\widetilde{\boldsymbol{K}}\widetilde{E}|\widehat{V}_{\rm p}|\boldsymbol{K}_0\rangle \\ &\quad + \sum_p \int \frac{\mathrm{d}\widetilde{E}_{\rm t}}{E_{\rm t} - \widetilde{E}_{\rm t} \pm \mathrm{i}0}\langle\lambda\boldsymbol{K}'|(\widehat{H}_{\rm t} - E_{\rm t})|p\widetilde{E}_{\rm t}\rangle\langle p\widetilde{E}_{\rm t}|\widehat{V}_{\rm p}|\boldsymbol{K}_0\rangle \\ &= t_{\mathrm{d1},\lambda}(\boldsymbol{K}'|\boldsymbol{K}_0) + t_{\mathrm{d2},\lambda}(\boldsymbol{K}'E|\boldsymbol{K}_0) + t_{\mathrm{c1},\lambda}(\boldsymbol{K}'E|\boldsymbol{K}_0). \end{aligned} \tag{A32}$$

That is, we account for direct AIS excitation, two-step excitation and correlation excitation through the adjacent continuum. Interaction with the projectile can thus be included through a Born-like expansion; however, we have neglected the third-order terms arising from two-step (second-Born) transitions to the continuum, since our earlier estimates (Godunov *et al* 1997b) and other results indicate that their contribution is small enough in the case of interest for this paper. Also, in the $t_{\mathrm{d}2,\lambda}$ amplitude, we have omitted transitions through the continuum, retaining only the states of one-electron excitation in the sum over intermediate states.

Equation (A32) can be treated as separating three components in the 'modified' vector of the open channel

$$|(\lambda E)\boldsymbol{K}'\rangle = |\lambda\boldsymbol{K}'\rangle + \sum_{p}\int \frac{\mathrm{d}\widetilde{E}_{\mathrm{t}}}{E_{\mathrm{t}} - \widetilde{E}_{\mathrm{t}} \pm \mathrm{i}0}|p\widetilde{E}_{\mathrm{t}}\rangle\langle p\widetilde{E}_{\mathrm{t}}|(\widehat{H}_{\mathrm{t}} - E_{\mathrm{t}})|\lambda\boldsymbol{K}'\rangle$$
$$+ \sum_{b}\int \mathrm{d}\widetilde{\boldsymbol{K}}\int \frac{\mathrm{d}\widetilde{E}}{E - \widetilde{E} \mp \mathrm{i}0}|b\widetilde{\boldsymbol{K}}\widetilde{E}\rangle\langle b\widetilde{\boldsymbol{K}}\widetilde{E}|\widehat{V}_{\mathrm{p}}|\lambda\boldsymbol{K}'\rangle \qquad \text{(A33)}$$

the second term corresponding to the admixture of the continuum though correlation well known from photoionization studies, and the last term representing the admixture of the continuum through the interaction with the charged projectile.

Avoiding the poorly tractable procedure of constructing prediagonalized continuum states $|a\boldsymbol{K}E\rangle$, we could restrict ourselves to the first-order treatment, as described in Ivanov and Safronova (1992), so that

$$|a\boldsymbol{K}E\rangle = |a\boldsymbol{K}E[0]\rangle + \sum_{b}\int \mathrm{d}\widetilde{\boldsymbol{K}}\int \frac{\mathrm{d}\widetilde{E}}{E - \widetilde{E} \mp \mathrm{i}0}|b\widetilde{\boldsymbol{K}}\widetilde{E}[0]\rangle\langle b\widetilde{\boldsymbol{K}}\widetilde{E}[0]|\widehat{V}|a\boldsymbol{K}E\rangle \qquad \text{(A34)}$$

with some primary basis $|a\boldsymbol{K}E[0]\rangle$ and residual interaction $\widehat{V}$. One choice is to use plane waves for the scattered projectile and $\widehat{V}_{\mathrm{p}}$ instead of $\widehat{V}$, which would result in a second-Born calculation (Godunov *et al* 1998). However, this approximation gives a poor asymptotic for continuum wavefunctions in the region of strong post-collision interaction, where one could use some closed solution of the three-particle equations of motion preserving collision kinematics—for instance, Faddeyev–Mercuriev wavefunctions (Godunov *et al* 1989). In the latter case, using (A34) we would encounter the hard problem of correctly determining the residual interaction, and most work in this direction, including this paper, did not involve first-order final-state corrections.

References

Åberg T and Howat G 1982 Theory of the Auger effect *Handbuch für Physik* vol 31, ed W Mehlhorn (Berlin: Springer) pp 469–619

Arcuni P W and Schneider D 1987 *Phys. Rev.* A **36** 3059–70

Bachau H, Gayet R, Hanssen J and Ourdane M A 1997 *Proc. 20th Int. Conf. on Physics of Electronic and Atomic Collisions (Vienna)* ed F Aumayr and H Winter, theorem 123

Balashov V V, Grishanova S I, Kruglova I M and Senashenko V S 1968 *Phys. Lett.* A **27** 101–2

Barker R B and Berry H W 1966 *Phys. Rev.* **151** 14–19

Bodea D, Orbán A, Ristoiu D and Nagy L 1998 *J. Phys. B: At. Mol. Opt. Phys.* **31** L745–55

Bordenave-Montesquieu A, Benoit-Cattin P, Rodière M, Gleizes A and Merchez H 1975 *J. Phys. B: At. Mol. Phys.* **8** 874–94

Breit G and Wigner E P 1936 *Phys. Rev.* **49** 519

Burke P G 1965 *Adv. At. Mol. Phys.* **14** 521–67

Crooks G B and Rudd M E 1970 *Phys. Rev. Lett.* **25** 1599–601

Fano U 1961 *Phys. Rev.* **124** 1866–78

Fano U and Cooper J W 1963 *Phys. Rev.* A **137** 1364–79

Fano U and Prats F 1963 *Proc. Natl Acad. Sci. India* A **33** 553–62
Gayet R, Hanssen J and Jacqui L 1995 *J. Phys. B: At. Mol. Opt. Phys.* **28** 2193–208
Godunov A L and Ivanov P B 1999 *Phys. Scr.* **59** 277–85
Godunov A L, Ivanov P B and Schipakov V A 1997a *J. Phys. B: At. Mol. Opt. Phys.* **30** 3403–15
Godunov A L, Kunikeev Sh D, Novikov N V and Senashenko V S 1989 *Sov. Phys.–JETP* **69** 927–33
Godunov A L, McGuire J H and Schipakov V A 1997b *J. Phys. B: At. Mol. Opt. Phys.* **30** 3227–45
Godunov A L, Novikov N V and Senashenko V S 1990 *J. Phys. B: At. Mol. Opt. Phys.* **23** L359–64
Godunov A L, Schipakov V A, Moretto-Capelle P, Bordenave-Montesquieu D, Benhenni M and Bordenave-Montesquieu A 1997c *J. Phys. B: At. Mol. Opt. Phys.* **30** 5451–77
Godunov A L, Schipakov V A and Schulz M 1998 *J. Phys. B: At. Mol. Opt. Phys.* **31** 4943–60
Godunov A L, Senashenko V S and Schipakov V A 1992 *Preprint* I V Kurchatov Institute of Atomic Energy IAE-5451/12 (Moscow) 1–55
Heideman H G M and van de Water W 1981 *Comment. At. Mol. Phys.* **10** 87–98
Howat G, Åberg T and Goscinski O 1978 *J. Phys. B: At. Mol. Phys.* **11** 1575–88
Itoh A, Zouros T J M, Schneider D, Stettner U, Zeitz W and Stolterfoht N 1985 *J. Phys. B: At. Mol. Phys.* **18** 4581–7
Ivanov P B 1989 Spectral characteristics of the autoionising states of two-electron systems *PhD Thesis* Institute of Spectroscopy, Academy of Sciences USSR
Ivanov P B and Safronova U I 1992 *J. Phys. B: At. Mol. Opt. Phys.* **25** 23–39
Ivanov P B and Senashenko V S 1983 *Autoionization Phenomena in Atoms and Ions* ed U I Safronova (Moscow) pp 34–73
Junker B R 1985 Complex stabilization method *Autoionization: Recent Development and Applications* ed A Temkin pp 103–33
Krause M O, Cerrina F and Fahlman A 1983 *Phys. Rev. Lett.* **50** 1118–21
Kuchiev M Yu and Scheinerman S A 1988 *J. Phys. B: At. Mol. Opt. Phys.* **21** 2027–38
Mandl F 1966 *Proc. Phys. Soc.* **87** 871–4
Moretto-Capelle P, Benhenni M, Bordenave-Montesquieu D and Bordenave-Montesquieu A 1996 *J. Phys. B: At. Mol. Opt. Phys.* **29** 2007–20
Moretto-Capelle P, Bordenave-Montesquieu D, Bordenave-Montesquieu A, Godunov A and Schipakov V 1997 *Phys. Rev. Lett.* **79** 5230–3
Ramaker D E 1971 The $(nl^2)^1$S autoionizing states of helium *PhD Thesis* University of Iowa, Iowa City, USA
Ramaker D E and Schraeder D M 1974 *Phys. Rev.* A **9** 1980–91
Reed M and Simon B 1978 *Methods of Modern Mathematical Physics. IV: Analysis of Operators* (New York: Academic)
Schowengerdt F D and Rudd M E 1972 *Phys. Rev. Lett.* **28** 127–30
Shore B W 1968 *Phys. Rev.* **171** 43–54
Schulz M, Htwe W T, Gaus A D, Peatcher J L and Vajnai T 1995 *Phys. Rev.* A **51** 2140–50
Starace A F 1977 *Phys. Rev.* A **16** 231–42
Stolterfoht N 1987 *Phys. Rep.* **146** 315–424